Supporting Information for Consequences of Grafting Density on Linear Viscoelastic Behavior of Graft Polymers

Ingrid N. Haugan,[1] Michael J. Maher,[1] Alice B. Chang,[2] Tzu-Pin Lin,[2] Robert H. Grubbs,[2] Marc A. Hillmyer,[3] and Frank S. Bates[1]

[1]Department of Chemical Engineering and Materials Science, University of Minnesota Twin Cities, Minneapolis, MN 55455, United States
[2]Division of Chemistry and Chemical Engineering, California Institute of Technology, Pasadena, CA 91125, United States

[3]Department of Chemistry, University of Minnesota Twin Cities, Minneapolis, MN 55455, United States

Table of Contents

All primary data files are available at https://doi.org/10.13020/D6T97M.

1. Synthesis of model materials

1.1 Materials

All chemicals were used as received unless otherwise noted. The second-generation Grubbs catalyst [$(H_2IMes)(PCy_3)(Cl)_2Ru$=CHPh] was generously supplied by Materia Inc., and the third-generation derivative **G3** [$(H_2IMes)(pyr)_2(Cl)_2Ru$=CHPh] was prepared according to the reported procedure.[1] 2-aminoethanol, ethyl vinyl ether, and racemic 3,6-dimethyl-1,4-dioxane-2,5-dione (lactide) were purchased from Sigma Aldrich. Carbic anhydride was purchased from Acros Organic, and tin (II) 2-ethylhexanoate (96%) was purchased from Alfa Aesar. Anhydrous dichloromethane was obtained from a solvent purification system, degassed, and stored in a glovebox.

1.2 Synthesis of PLA macromonomer

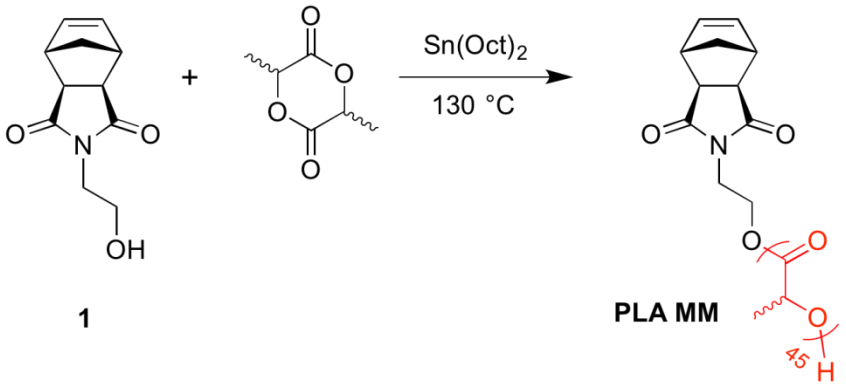

The ω-norbornenyl poly(±-lactide) macromonomer was synthesized according to reported procedures.[2,3] A flame-dried Schlenk flask was charged with a stir bar, initiator **1** (2.00 g, 9.65 mmol, 1.00 equiv), and racemic 3,6-dimethyl-1,4-dioxane-2,5-dione (29.2 g, 203 mmol, 21.0 equiv). The flask was subjected to three pump-purge cycles using argon, then transferred to an oil bath heated to 130 °C. Once the contents of the flask had fully melted (approx. 0.5 hr), one drop of the catalyst, tin (II) 2-ethylhexanoate (≈ 5 mg), was added using a 21G needle. The reaction was allowed to stir at 130 °C for 4 hr, then quenched by rapidly cooling in a dry ice bath. The solid was dissolved in dichloromethane, and then the solution was filtered through basic alumina to remove the tin catalyst. The solution was concentrated by rotary evaporation until slightly viscous, then precipitated dropwise to stirring cold (−78 °C) methanol. The solid was isolated by centrifugation and dried under high vacuum to yield the PLA macromonomer as a white crystalline solid. ^{1}H NMR end group analysis: M_n = 3450 g/mol.

Sample ID	z	M_w (kg/mol)	n_{bb}[a]	Dispersity	T_g (°C)	η_0 (10^3 Pa·s)

1.3 General procedure for graft polymer ROMP synthesis

All graft polymers were synthesized by ring-opening metathesis polymerization (ROMP) according to reported procedures.[4] Analysis of the homo- and copolymerization kinetics of the PLA macromonomer and DME diluent indicate ideal random copolymerization and therefore uniform incorporation throughout the backbone (r_1 = 0.89, r_2 = 1.13, r_1r_2 = 1.01). Each sample was synthesized on at least a 250 mg scale. In an argon glovebox, the appropriate amount of the PLA macromonomer (3450 g/mol) was transferred to a 4 mL vial charged with a stir bar. For each grafting density series, a stock solution of the DME diluent in dichloromethane was prepared such that [DME] = [(1−z) / z] × [PLA], where the macromonomer concentration was fixed for all z: [PLA] = 0.05 M. The appropriate volume of the diluent stock solution was added to each reaction vial in order to obtain the target initial value of [PLA]. For each sample, an aliquot of the comonomer mixture (≈ 20 μL) was collected and analyzed by ^{1}H NMR in order to confirm the grafting densities (Section 2.1).

A stock solution of the third-generation Grubbs catalyst **G3** [$(H_2IMes)(pyr)_2(Cl)_2Ru$=CHPh] was prepared in dichloromethane. Each polymerization was initiated by addition of an appropriate volume of the catalyst stock solution while stirring vigorously. After 1 hour, the polymerizations were quenched by rapid addition of a large excess of ethyl vinyl ether (≈ 0.2 mL) and a silica-bound metal scavenger (SiliaMetS). Removing the quenched ruthenium complex from solution prevents potential reactivation and undesired metathesis. The graft polymers were precipitated through a syringe filter by dropwise addition into 50 mL cold (−78 °C) methanol. Samples were isolated by centrifugation, then dried under high vacuum for 24 hours. Samples were lyophilized from benzene in order to remove residual solvent. Subsequent analysis by SEC enables determination of the total backbone degree of polymerization, n_{bb} (Section 2.2).

The molecular and thermal data for all of the model polymers are summarized in Table S1.

Table S1. Molecular and thermal characterization of graft polymers.

$(PLA)_{12}$	1.00	40.3	12	1.04	54	6.1
$(PLA)_{24}$	1.00	81.6	24	1.01	53	12
$(PLA)_{55}$	1.00	189	55	1.01	52	18
$(PLA)_{97}$	1.00	335	97	1.03	52	39
$(PLA)_{200}$	1.00	676	200	1.03	52	94
$(PLA)_{510}$	1.00	1770	510	1.05	53	270
$(PLA)_{1100}$	1.00	3960	1100	1.10	54	540
$(PLA)_{2900}$	1.00	10000	2900	1.37	51	30000
$(PLA^{0.5}$- *ran* -$DME^{0.5})_{22}$	0.50	40.7	22	1.04	53	9.0
$(PLA^{0.5}$- *ran* -$DME^{0.5})_{85}$	0.50	156	85	1.02	52	22
$(PLA^{0.5}$- *ran* -$DME^{0.5})_{460}$	0.50	840	460	1.04	53	170
$(PLA^{0.5}$- *ran* -$DME^{0.5})_{960}$	0.50	1760	960	1.06	54	620
$(PLA^{0.5}$- *ran* -$DME^{0.5})_{2600}$	0.50	4840	2600	1.13	53	4600
$(PLA^{0.4}$- *ran* -$DME^{0.6})_{440}$	0.40	658	440	1.04	52	--
$(PLA^{0.4}$- *ran* -$DME^{0.6})_{1600}$	0.40	2440	1600	1.11	51	--
$(PLA^{0.25}$- *ran* -$DME^{0.75})_{40}$	0.25	41.2	40	1.04	53	7.3
$(PLA^{0.25}$- *ran* -$DME^{0.75})_{62}$	0.25	63.2	62	1.02	52	17
$(PLA^{0.25}$- *ran* -$DME^{0.75})_{88}$	0.25	90.0	88	1.01	54	16
$(PLA^{0.25}$- *ran* -$DME^{0.75})_{130}$	0.25	133	130	1.02	53	33
$(PLA^{0.25}$- *ran* -$DME^{0.75})_{210}$	0.25	217	210	1.01	53	55
$(PLA^{0.25}$- *ran* -$DME^{0.75})_{270}$	0.25	276	270	1.02	53	100
$(PLA^{0.25}$- *ran* -$DME^{0.75})_{330}$	0.25	341	330	1.02	53	120
$(PLA^{0.25}$- *ran* -$DME^{0.75})_{410}$	0.25	417	410	1.02	53	190
$(PLA^{0.25}$- *ran* -$DME^{0.75})_{640}$	0.25	650	640	1.03	54	450
$(PLA^{0.25}$- *ran* -$DME^{0.75})_{840}$	0.25	855	840	1.03	53	880
$(PLA^{0.25}$- *ran* -$DME^{0.75})_{1500}$	0.25	1480	1500	1.07	54	5100
$(PLA^{0.25}$- *ran* -$DME^{0.75})_{1800}$	0.25	1850	1800	1.11	53	12000
$(PLA^{0.2}$- *ran* -$DME^{0.8})_{120}$	0.20	103	120	1.02	52	--
$(PLA^{0.2}$- *ran* -$DME^{0.8})_{1100}$	0.20	905	1100	1.04	53	--
$(PLA^{0.15}$- *ran* -$DME^{0.85})_{88}$	0.15	60.9	88	1.02	55	25
$(PLA^{0.15}$- *ran* -$DME^{0.85})_{170}$	0.15	116	170	1.01	56	100
$(PLA^{0.15}$- *ran* -$DME^{0.85})_{420}$	0.15	292	420	1.02	55	1600
$(PLA^{0.15}$- *ran* -$DME^{0.85})_{720}$	0.15	501	720	1.03	56	12000
$(PLA^{0.15}$- *ran* -$DME^{0.85})_{1500}$	0.15	1010	1500	1.04	53	200000
$(PLA^{0.05}$- *ran* -$DME^{0.95})_{200}$	0.05	76.1	200	1.01	59	130
$(PLA^{0.05}$- *ran* -$DME^{0.95})_{410}$	0.05	154	410	1.01	59	1200
$(PLA^{0.05}$- *ran* -$DME^{0.95})_{950}$	0.05	352	950	1.02	59	14000
$(DME)_{100}$	0	20.1	100	1.01	83	8.1
$(DME)_{200}$	0	41.2	200	1.01	89	55
$(DME)_{510}$	0	107	510	1.01	88	200
$(DME)_{900}$	0	188	900	1.01	89	11000

[a] n_{bb} is calculated from weight-average molar mass.

2. Characterization of graft polymers

All of the polymers were characterized by ^{1}H NMR, SEC, DSC, SAXS, and rheology. Characteristic data (for the z = 0.15 series) for each technique are shown below and are representative for all polymers (unless otherwise explicitly stated). Data for all polymers are shown in Section 5.

2.1 ^{1}H NMR of comonomer mixtures to determine grafting density

For each sample, an aliquot of the macromonomer/diluent mixture was collected prior to initiating the polymerization. The grafting density was determined from the relative ^{1}H NMR integrations of the olefin resonances for the PLA macromonomer (6.30–6.25 ppm) and the discrete diluent (6.30–6.25, 6.10–6.05 ppm). Because the diluent resonances are centrosymmetric (*ddd*), the molar equivalents of the macromonomer and diluent are directly obtained by comparison. In turn, the grafting density is obtained from the mole fraction of the macromonomer. Representative spectra and calculations for the z = 0.15 series are provided in Figure S1 and Table S2. For all samples, the calculated grafting densities were within 3% of the target values.

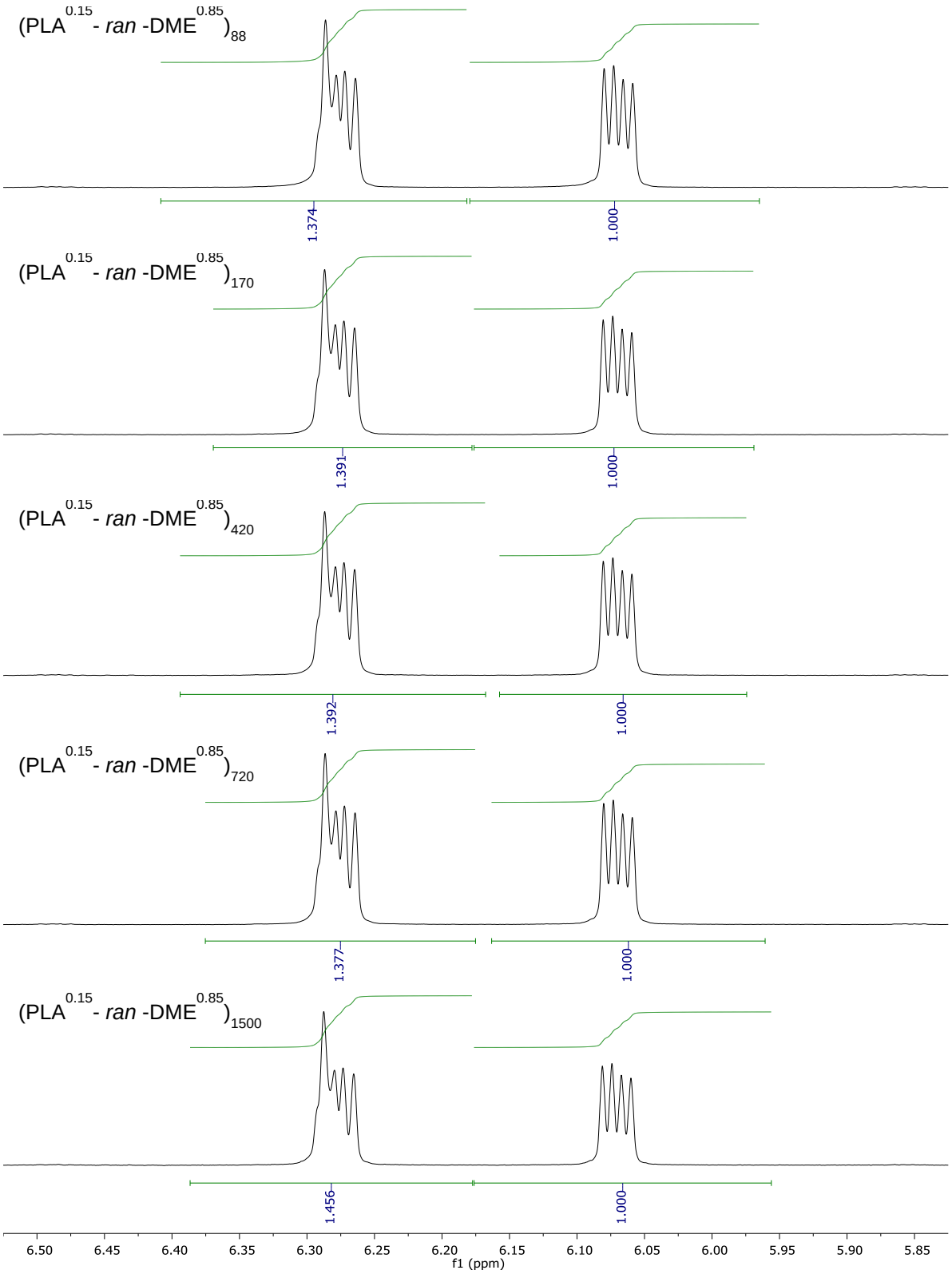

Figure S1. ^{1}H NMR spectra of the comonomer mixtures for each z = 0.15 sample prior to initiation.

Table S2. Representative calculations for the grafting density of each z = 0.15 sample from ^{1}H NMR analysis.

Sample ID	Integration (6.30–6.25 ppm)	Integration (6.10–6.05 ppm)	Equiv. MM	Equiv. DME	z
$(PLA^{0.15}\text{-}ran\text{-}DME^{0.85})_{88}$	1.37	1.00	0.37	2.00	0.158
$(PLA^{0.15}\text{-}ran\text{-}DME^{0.85})_{170}$	1.39	1.00	0.39	2.00	0.164
$(PLA^{0.15}\text{-}ran\text{-}DME^{0.85})_{420}$	1.39	1.00	0.39	2.00	0.164
$(PLA^{0.15}\text{-}ran\text{-}DME^{0.85})_{720}$	1.38	1.00	0.38	2.00	0.159
$(PLA^{0.15}\text{-}ran\text{-}DME^{0.85})_{1500}$	1.45	1.00	0.45	2.00	0.185

2.2 Size exclusion chromatography (SEC) to determine n_{bb}

SEC data were collected using two Agilent PLgel MIXED-B 300 × 7.5 mm columns with 10 μm beads, connected to an Agilent 1260 Series pump, a Wyatt 18-angle DAWN HELEOS light scattering detector, and Optilab rEX differential refractive index detector. The mobile phase was tetrahydrofuran. SEC data for the z = 0.15 series are provided in Figure S2. Data for all other graft polymers are provided in Section 5.

For each sample, a solution of known concentration (2 mg/mL) was injected. The dn/dc values were determined by online measurements assuming 100% mass elution under the peak of interest. For all samples of the same grafting density, the dn/dc values were averaged and used to determine the weight-average total backbone degrees of polymerization, n_{bb}.

n_{bb} is the sum of the weight-average backbone degrees of polymerization of the PLA macromonomer and DME diluent (n_{PLA} and n_{DME}, respectively). The grafting density relates n_{PLA} and n_{DME}:

$$f = \frac{z}{1-z} = \frac{n_{\mathrm{PLA}}}{n_{\mathrm{DME}}} \tag{S1}$$

Eq. S1 can be introduced into an expression for the weight-average total molar mass, M_w:

$$M_{\mathrm{w}} = M_{\mathrm{PLA}} n_{\mathrm{PLA}} + M_{\mathrm{DME}} n_{\mathrm{DME}} = n_{\mathrm{DME}}(M_{\mathrm{PLA}} f + M_{\mathrm{DME}}) \tag{S2}$$

where M_{PLA} is the weight-average molar mass of the PLA macromonomer (3.45 kg/mol) and M_{DME} is the molar mass of the diluent (0.21 kg/mol). n_{DME} can be calculated using the M_w values determined by SEC:

$$n_{\mathrm{DME}} = \frac{M_{\mathrm{w}}\ (\mathrm{kDa})}{3.45f + 0.21} \tag{S3}$$

From Eqs. S1 and S3, n_{PLA} and n_{bb} follow.

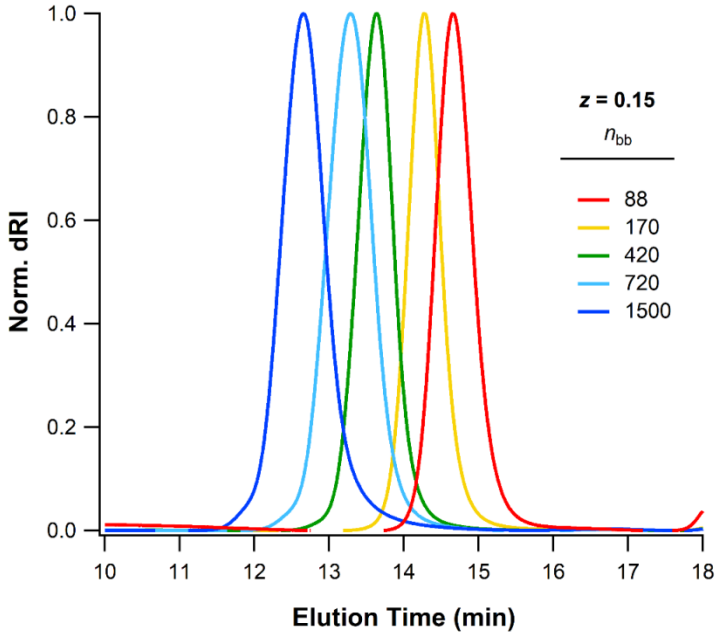

Figure S2. SEC data for all samples with z = 0.15.

2.3 Dynamic scanning calorimetry (DSC)

DSC data were collected using a TA Q1000 equipped with a TA LNCS under dry N_2. All polymers were dried under vacuum at elevated temperatures (> 100 °C) for several hours to remove any residual solvent prior to collecting data, and hermetically sealed at room temperature in ambient conditions using Tzero pans. All samples were heated between 0 and 220 °C at a rate of 10 °C/min. The data reported was collected on the second heating cycle. All samples showed a single T_g with no evidence of crystallization (as expected with the use of ±-lactide), as shown in Figure S3. The T_g in the limit of high M_w for each grafting density series is shown in Table S3.

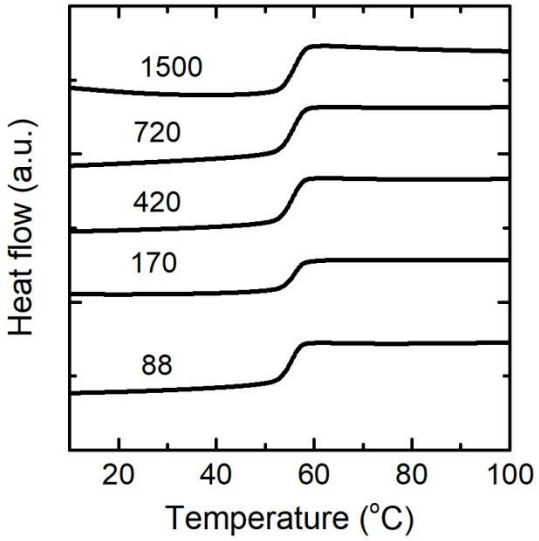

Figure S3. DSC traces for the z = 0.15 series, with n_{bb} labeled on graph. Curves were shifted for clarity.

Table S3. Approximate asymptotic T_g of each grafting density series.

z	Approximate T_g (°C)
1.00	53
0.50	53
0.40	51
0.25	53
0.20	53
0.15	56
0.05	59
0	89

2.4 Small-angle X-ray scattering (SAXS)

All SAXS data were collected at the Sector 5-ID-D Dow-Northwestern-Dupont beamline (Advanced Photon Source at Argonne National Laboratory). All polymers were dried under vacuum at elevated temperatures (> 100 °C) for several hours to remove any residual solvent, and bulk samples were mounted onto Kapton tape. Data was collected at room temperature with a photon wavelength of λ = 0.729 Å. The SAXS patterns for all of the samples showed no scattering indicative of microphase separation, as shown in Figure S4, indicating that all of the polymer samples formed homogeneous melts.

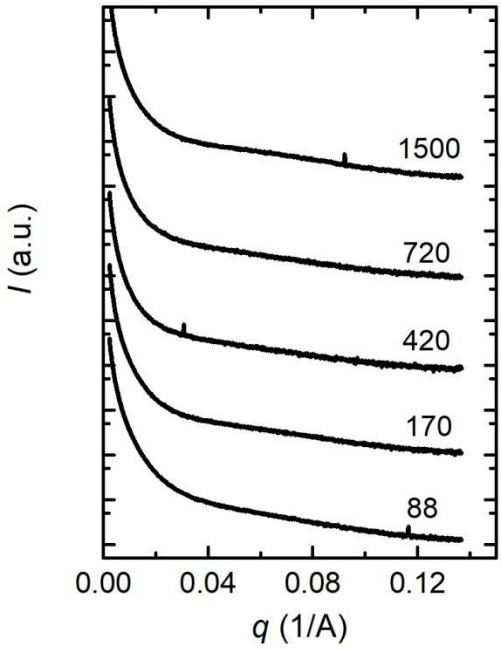

Figure S4. SAXS spectra for z = 0.15 series, arbitrarily shifted for clarity, and n_{bb} labeled on graph.

2.5 Linear rheology

All rheology data was collected using a Rheometric Scientific Ares 2 rheometer with temperature controlled by a forced convection oven. All samples were loaded onto 8 mm parallel plates and measured under dry nitrogen. Dynamic strain sweep analysis at 70 °C and 100 rad/s showed the linear viscoelastic regime persisted to 20% strain for all samples (linear DME samples were tested at 100 °C). Dynamic frequency sweep analysis was carried out from 70 to 200 °C (100–220 °C for linear DME samples) at a frequency range of 100–0.1 rad/s and a strain lower than the linear viscoelastic threshold. Master curves were prepared by shifting G^* along frequency axis to a reference of $T_{ref} = T_g + 34$ °C, an arbitrary temperature to compare values of η_0.[5]

3. Interpretation of results:

3.1 Thermorheological simplicity of graft polymers

All graft polymer demonstrated thermorheological simplicity as demonstrated by: 1) fit with WLF model, 2) continuous van Gurp-Palmen plots, 3) appearance of one T_g by DSC, and 4) no microphase separation as seen by SAXS.

3.1.1 Fit to WLF model

Shift factors were fitted to Williams-Landel-Ferry (WLF) model, and calculated by eq. S4

$$\log(a_T) = \frac{-C_1(T - T_{ref})}{C_2 + (T - T_{ref})} \quad \text{(S4)}$$

where a_T is the shift factor, C_1 and C_2 are the WLF parameters, and $T_{ref} = T_g + 34$ °C. Figure S5 shows the shift factor for the graft polymers, fit with WLF parameters $C_1 = 6.7$ and $C_2 = 78$ °C. All of the grafted polymers fit the same WLF parameters, even though volume fraction of the backbone drastically varied. This has been shown previously for bottlebrush polymers.[6]

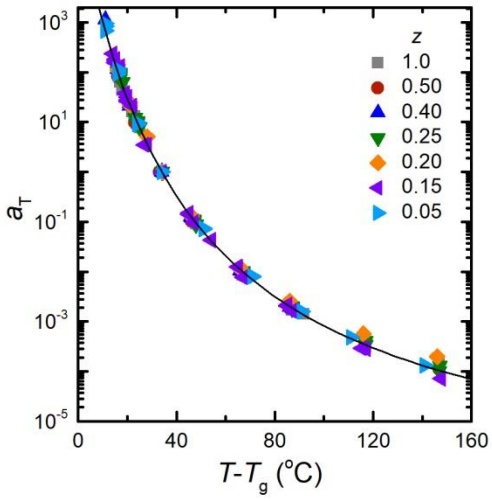

Figure S5. Shift factors for all graft polymers, with WLF parameters $C_1 = 6.7$ and $C_2 = 78$ °C for $T_{ref} = T_g + 34$ °C.

3.1.2 Van Gurp-Palmen plots

The van Gurp-Palmen (vGP) plot is classically used to determine if TTS is appropriate for a polymer melt.[7] Above the T_g, TTS fails when there are domains of different materials because domains could have varying monomeric friction factors, which govern thermal relaxations. The loss angle, δ, is calculated by Eq. S5.

$$\tan\delta = \frac{G''}{G'} \quad \text{(S5)}$$

The loss angle is used to determine is TTS works because δ should be invariant to temperature changes because the density differences are cancelled out by the ratio of G' to G''. Figure S6 shows the vGP plot for the $z = 0.15$ series. All of the traces are continuous, which is indicative of a thermorheologically simple melt.

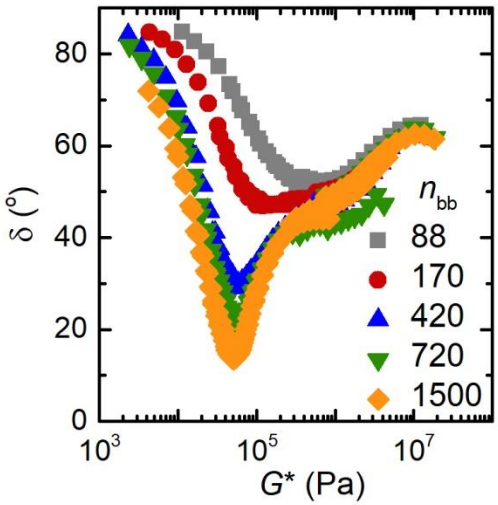

Figure S6. Van Gurp-Palmen plot for z = 0.15 series.

3.1.3 DSC and SAXS

As discussed previously, both the DSC traces and SAXS data show no microphase separation. The DSC traces, as shown in Figure S3, show only one T_g, whereas microphase-separated domains typically show two distinct T_g values corresponding to the two domains. The T_g of the two domains (53 °C for PLA and 89 °C for DME) should be separated enough to achieve distinct T_g values for microphase separated domains. Instead, there is one T_g for the material that reflects the composition of the polymer.

The SAXS traces show no scattering between different domains, as shown in Figure S4, further demonstrating that the polymer melt is homogeneous.

3.2 General Rheological Phenomena

3.2.1 Master curves

Master curves were prepared by shifting individual frequency sweeps by G^* along frequency axis to a reference of $T_{ref} = T_g + 34$ °C. Figure S7 shows a master curve for a representative (entangled) graft polymer sample. The data showed three regimes: 1) Rouse dynamics at high reduced frequency, 2) reptation dynamics at intermediate reduced frequency, and 3) terminal flow at low reduced frequency. Polymers below the critical molar mass (M_c) did not exhibit the second regime, but instead experienced a Rouse relaxation transition straight to terminal flow.

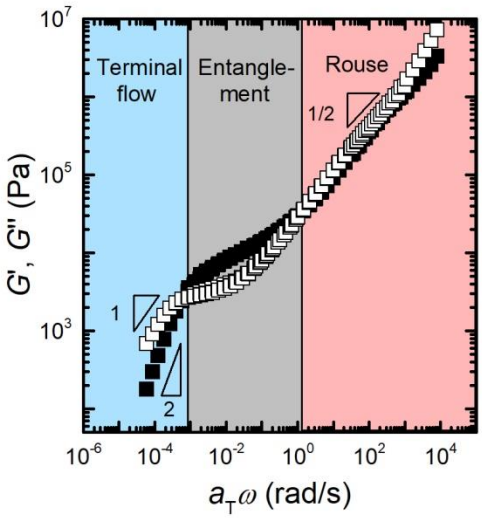

Figure S7. Master curve for (PLA$^{0.25}$-*ran*-DME$^{0.75}$)$_{1800}$ where G' is shown with closed symbols and G'' with open symbols. The Rouse regime is highlighted in pink, with a triangle to demonstrate G' and G'' both scaling as $\omega^{1/2}$. The entanglement region is highlighted in gray, where G' plateaus. Terminal flow is highlighted in blue, with triangles to demonstrate G' and G'' scaling as ω^2 and ω, respectively.

3.2.2 Zero-shear viscosity

The zero-shear viscosity, η_0, of materials was taken to be the value of η^*/a_T at the low frequency plateau for each polymer in the reduced viscosity versus reduced frequency plot, as shown in Figure S8. All values are referenced to $T_{ref} = T_g + 34$ °C, allowing η_0 values to be compared directly.

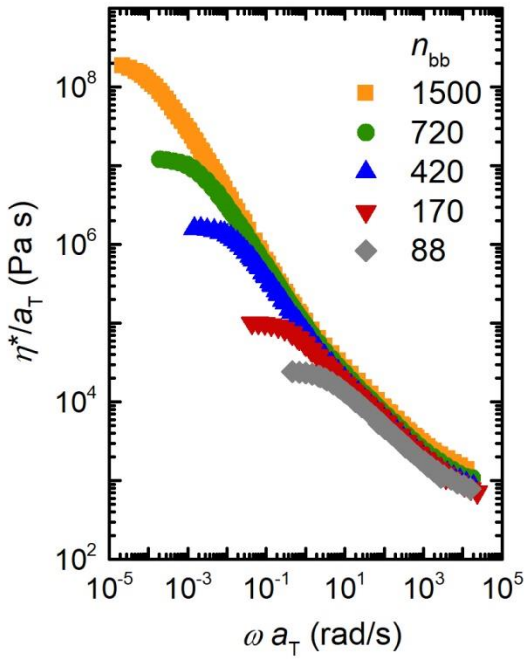

Figure S8. η^*/a_T for the z = 0.15 series.

3.2.3 Measuring M_e of graft polymers

The entanglement molar mass (M_e) was measured using the van Gurp-Palmen (vGP) method.[7] G_e is taken as G^* as $\delta \rightarrow 0°$. Graft polymers exhibit two relaxation modes in the vGP plot due to the relaxation of side chains and backbones. The relaxation of side chains yields a G_e similar to that of a linear polymer chain, and the relaxation of the backbone occurs at lower values of G^*;[8] for this experiment, G_e is taken as the value of G^* in the backbone regime.

The vGP plot, shown in Figure S9, of the largest sample in each grafting density series (the most entangled sample) was used to measure M_e for each series. G_e and M_e are independent of n_{bb} (given that the chain is long enough to exhibit entanglements), so n_{bb} was not kept constant when estimating these parameters. In addition, experimental limitations prohibited using a constant value of n_{bb}. Low z graft polymers with n_{bb} values comparable to the highest grafting density samples would not have a thermally accessible terminal flow regime because of anticipated thermal degradation of PLA. M_e was calculated according to Eq. S6:

$$M_e = \frac{\rho RT}{G_e} \tag{S6}$$

where ρ = 1.25 g/cm^3 and T was taken as T_{ref} for each sample. Figure S10 shows M_e vs z as calculated according to Eq. S6.

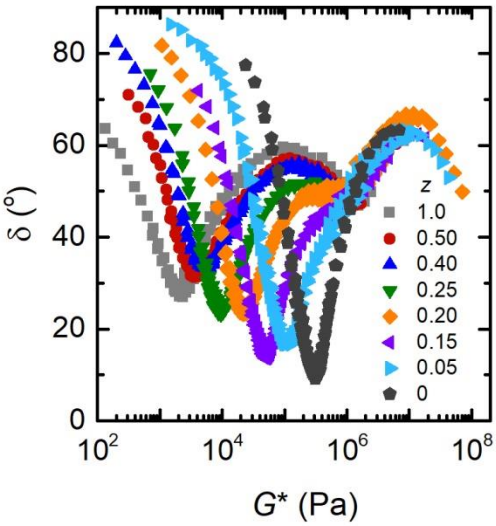

Figure S9. Van Gurp-Palmen plot for the largest sample in each grafting density series.

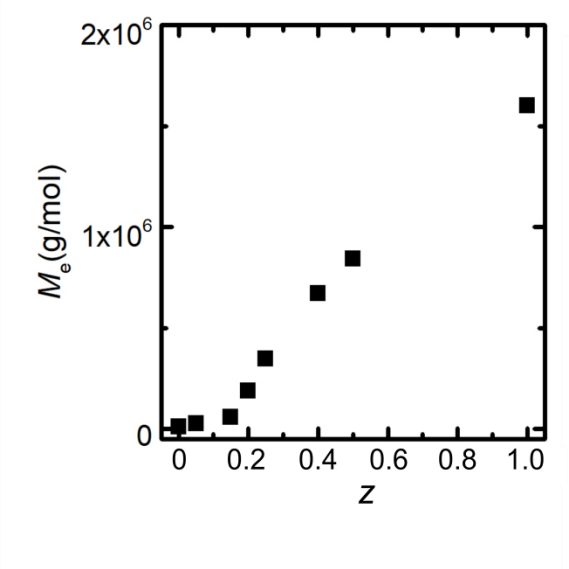

Figure S10. M_e *vs.* z as calculated using vGP plot and Eq. S6.

All of the samples in Figure S9 have a minimum δ value below 40°, which is indicative of entanglement (below 45°). Figure S11 shows master plots for all of the samples used to calculate M_e to demonstrate that they all exhibit entanglement plateaus. However, the lower z samples were much more entangled, as evidenced by their lower δ values. To evaluate the error in the estimating G_e at higher values of δ, the three entangled samples in the z = 0.15 series (Figure S6) were evaluated; their minimum δ values are 29.0, 20.9, and 13.6°. The values of G_e range from 51,500 to 54,200 Pa and are within a 5% error of each other. We conclude that estimating G_e from samples with a δ value below 40° is precise within 5%.

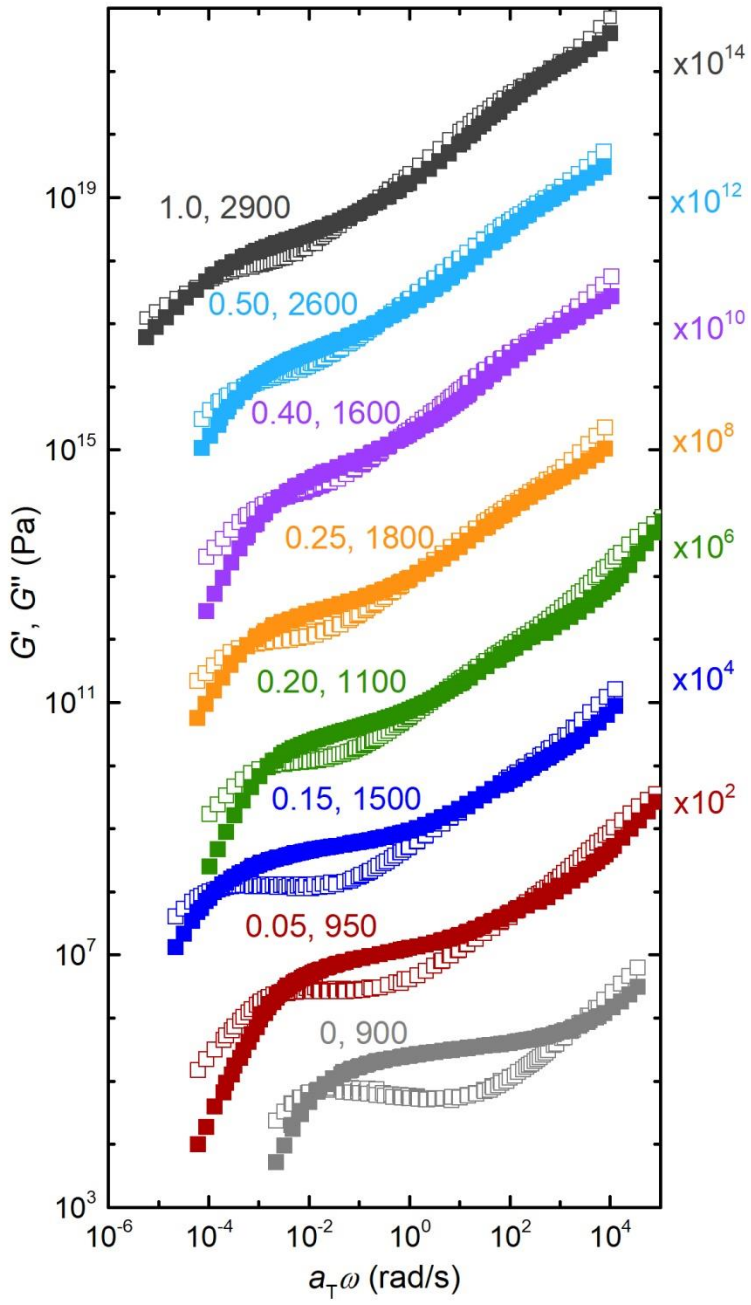

Figure S11. Master plots for each sample used to calculate M_e. Master curves are directly labelled with z, n_{bb} for the corresponding sample. Master curves are shifted arbitrarily for clarity, with shift factos labelled on the right.

The number of backbone units between entanglements, $n_{e,bb}$, was calculated from M_e according to Eq. S7:

$$n_{e,bb} = M_e \frac{z^{-1}}{M_{n,sc} + M_{n,bb}(z^{-1} - 1)} \quad \text{(S7)}$$

where z^{-1} is the number of backbone units between grafts (inverse grafting density, *not* volume normalized), $M_{n,sc}$ is the side chain molar mass, and $M_{n,bb}$ is the molar mass of one backbone unit. The values of M_e and $n_{e,bb}$ are listed for each grafting density in Table S4. The samples were determined to be entangled if the master curves showed an entanglement plateau, $M_w > 2\ M_e$, and the vGP plot showed a minimum below $\delta = 45$ °.

Table S4. M_e and $n_{e,bb}$ for each grafting density.

z	M_e (g/mol)	$n_{e,bb}$
1.0	$1.6\ 10^6$	550
0.50	$8.4\ 10^5$	460
0.40	$6.7\ 10^5$	441
0.25	$3.5\ 10^5$	340
0.20	$1.9\ 10^5$	220
0.15	$5.8\ 10^4$	86
0.05	$2.9\ 10^4$	78
0	$1.1\ 10^4$	55

4. Application of theory to experimental results

4.1 Important variables

4.1.1 Graft polymer variables

There are several important variables to define for graft polymers. Previously we have defined side chain length (n_{sc}), backbone length (n_{bb}), and grafting density (z). The scaling theory proposed by Rubinstein *et al.*[9] used several variables to define the space filling of the graft polymers. While intuitive, the grafting density does not reflect a chain length. Instead, the number of volume-normalized backbone units between grafts (n_g) is used as an analog to n_{sc}. Rubinstein *et al*. also use the Kuhn length (l_k), monomer contour length (l), and monomer volume (v_{ref}) to in their scaling theory; these three variables were assumed to be equal for the backbone and the side chains. We have used the monomer volume 118 Å^3.

In our analysis, we use statistical segment length (b) in place of the Kuhn length and monomer contour length, with the relation following Eq. S8.

$$b = \sqrt{l_k\, l} \tag{S8}$$

We take b for PLA to be 7.0 Å.[10] If we assume that $b_{DME} = b_{PLA}$, and that l = 5 Å, we calculate that l_k = 10 Å, corresponding to two norbornene units. Previous theory typically assumes that these scaling laws hold when $n_g >> l_k$, but that is not necessarily true for our polymers at the transitions.

4.1.2 Calculating chain dimensions

The radius of gyration of the PLA side chains was calculated assuming an unperturbed Gaussian coil, calculated according to Eq. S9.

$$R_g = \sqrt{\frac{n_{ref}}{6}}\, b \tag{S9}$$

where n_{ref} is the degree of polymerization normalized to a reference volume of v_{ref} = 118 Å^3 and b_{PLA} = 7.0 Å.[10] This gives a value of 17.4 Å for the 3,300 g/mol side chain (accounting for the 210 g/mol norbornene end group). Here we used only the PLA portion of the $M_{n,sc}$ to calculate side chain R_g.

The length between grafts was calculated according to Eq. S10.

$$L_g = l\, n_g \tag{S10}$$

We make the assumption that the backbone is completely extended and that the contour length per backbone unit is constant,[11] l = 5 Å.

4.2 Change in conformation with grafting density

The conformation of the backbone is important to the way that it fills space, and as such, entangles. Fetters *et al.* developed a relationship between the conformation of the backbone and the entanglement modulus.[12] We have modified this equation to calculate the statistical segment length in place of C_∞. This is not a quantitative calculation for b because it is based on the monomer unit rather than a volume unit. However, the data for b are consistent for all of the samples, so a qualitative comparison of b *vs.* z is valid. The statistical segment length of the backbone was calculated by the packing length argument according to Eqs. S11 and S12.

$$G_e = (A')^2 \frac{kT}{(p^*)^3} \tag{S11}$$

$$p^* = \frac{M_{n,bb}}{\rho N_A C_\infty l^2} = \frac{M_{n,bb}}{\rho N_A (\frac{n_{bb}}{N_c}) b^2} \tag{S12}$$

where A' is equal to 0.0595,[12] p^* is the packing length, N_C is the number of carbon bonds, and N_A is the Avogadro constant. The statistical segment length calculated here is referenced to one backbone unit (N/n = 5) rather than the reference volume, 118 Å^3. This allows us to compare the b vs z for our data, but these calculations should not be taken as quantitative values. The results for b vs z are shown in Figure S12.

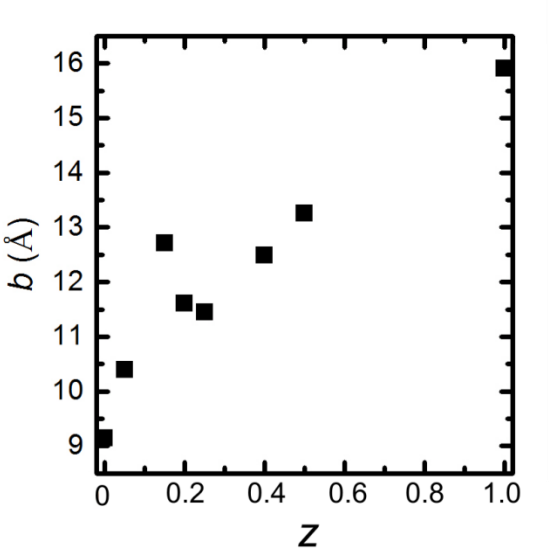

Figure S12. Statistical segment length vs grafting density for graft polymers as calculated by Eqs. S11 and S12.

In the low and high grafting density limits (LC and DB regimes), the statistical segment length increases with increasing grafting density. This is unexpected because the backbone is traditionally thought to stiffen with increasing grafting density. However, at intermediate grafting density, *b* drops suddenly. This is consistent with the argument that the backbone becomes more "flexible" (lower value of *b*) in the intermediate grafting density regime. Figure S13 shows a sketch of the proposed backbone kinking that results in a more "flexible" chain, which is similar to the torsional limitations that Lin *et al*. observed.[13]

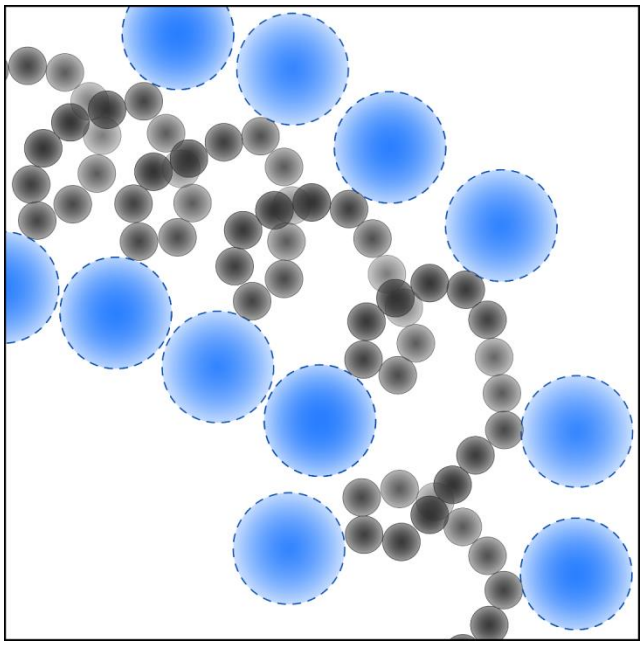

Figure S13. Cartoon depiction of backbone folding back on itself to space out side chains.

4.3 Coordination number of side chains

The coordination number, or the number of side chains that can fit in the pervaded space of one side chain, is very important to the theory proposed by Rubinstein *et al.*[9] Here, we estimate the coordination number, *C*, according to Eq. S13.

$$C = \frac{V_{\text{pervaded}}}{V_{\text{occupied}}} \tag{S13}$$

where

$$V_{\text{pervaded}} = \frac{4}{3}\pi R_{\text{g}}^3 \tag{S14}$$

$$V_{\text{occupied}} = \frac{M_{\text{w}} \times 10^{24}}{\rho N_{\text{A}}} \tag{S15}$$

Using values of R_g = 17.4 Å and ρ = 1.25 g/cm^3, we obtain $C \approx 5$.

5. Data for all grafting density samples

The data shown here is grouped by grafting density: *z* = 1.00, 0.50, 0.40, 0.25, 0.20, 0.15, 0.05, and 0. For each series, the data shown includes the following: SEC traces, master curve, η^*/a_T vs $a_T\omega$, van Gurp-Palmen plot, shift factors, DSC traces, and SAXS data.

5.1 z = 1.00 data

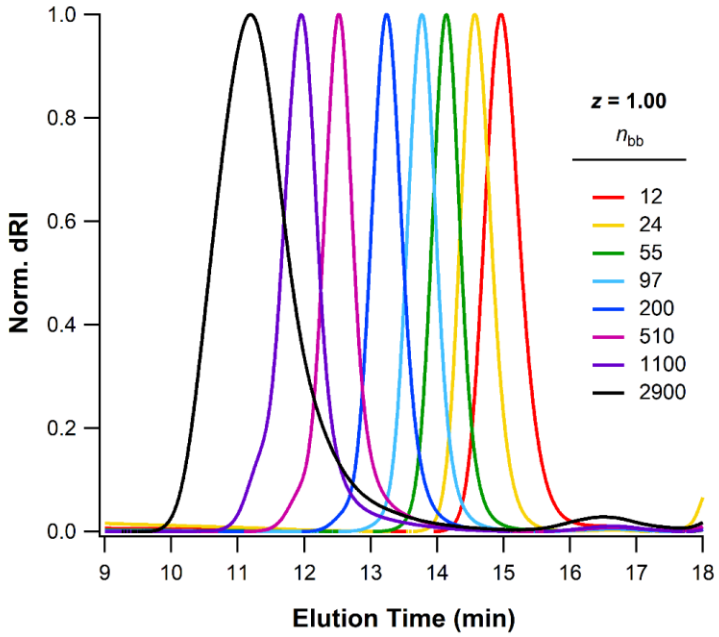

Figure S14. SEC data for all samples with *z* = 1.00.

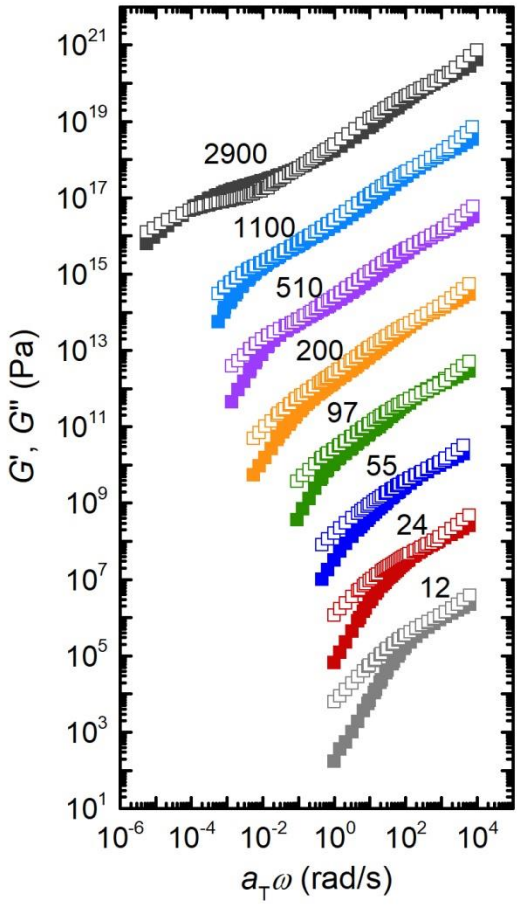

Figure S15. Master curves for z = 1.00 series, with n_{bb} labeled on graph. Master curves have been arbitrarily shifted for clarity.

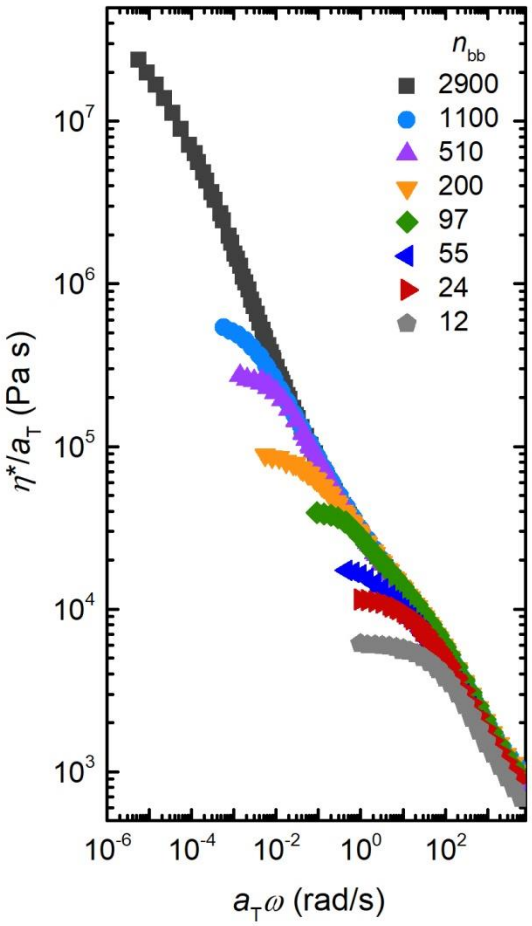

Figure S16. Reduced shear viscosity versus reduced frequency for z = 1.00series.

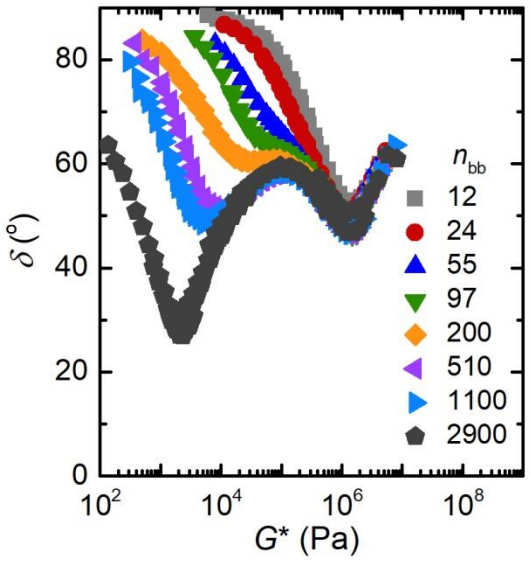

Figure S17. Van Gurp-Palmen plot for z = 1.00 series.

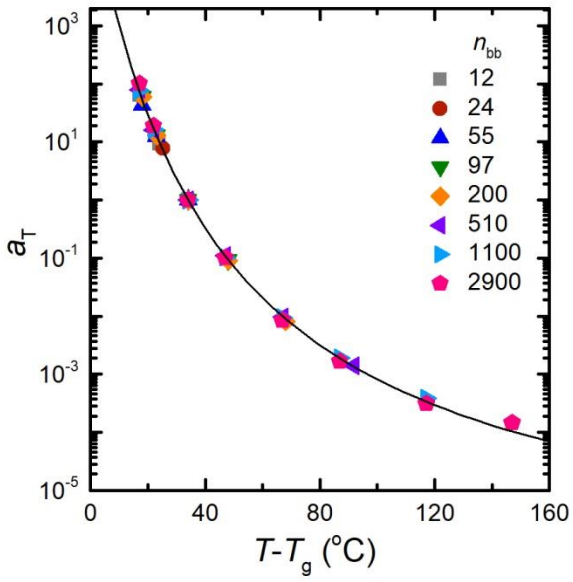

Figure S18. Shift factors for z = 1.00polymers with WLF parameters C_1 = 6.7 and C_2 = 78 °C for $T_{ref} = T_g + 34$ °C.

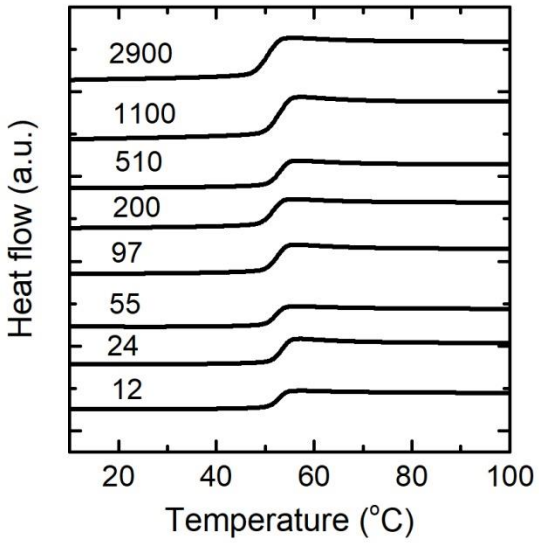

Figure S19. DSC traces for z = 1.00 series.

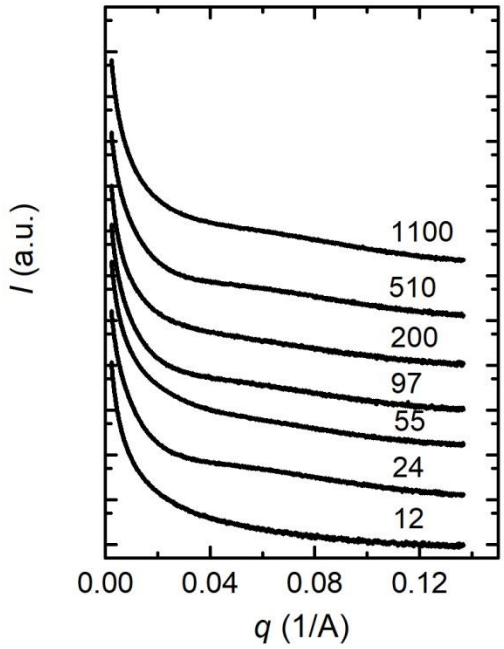

Figure S20. SAXS data for z = 1.00 series. $(PLA)_{2900}$ was not included in SAXS measurement.

5.2 z = 0.50 data

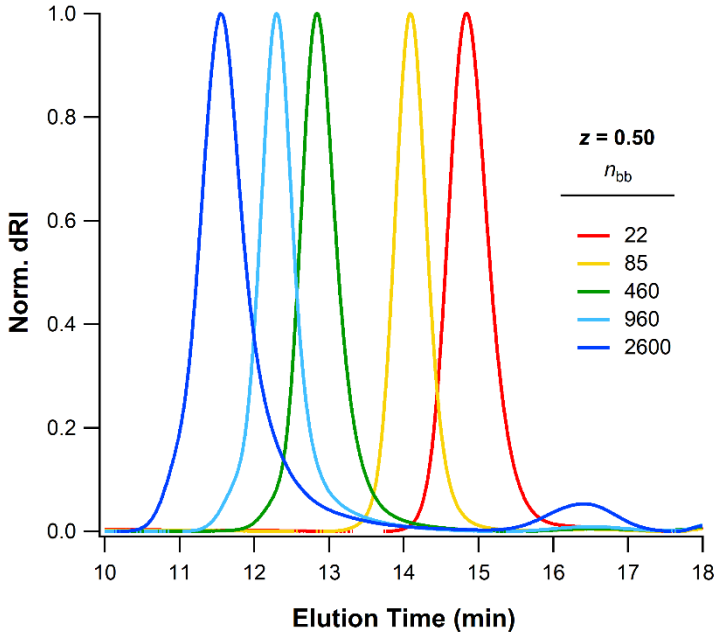

Figure S21. SEC data for all samples with z = 0.50.

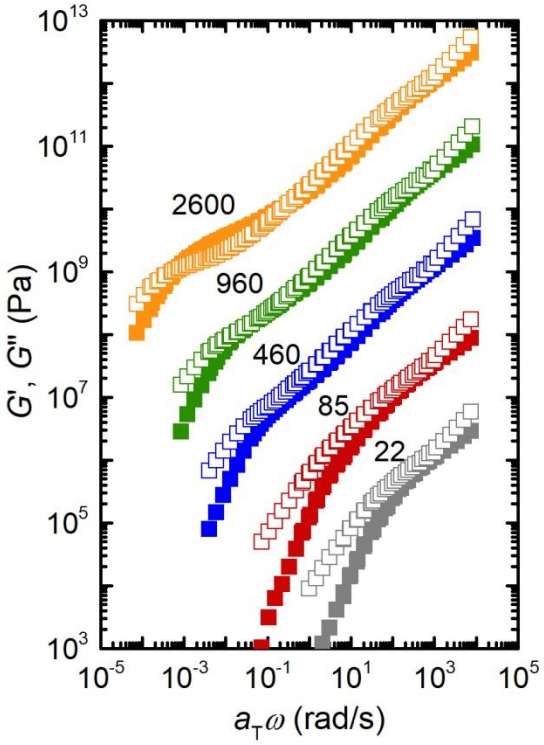

Figure S22. Master curve for z = 0.50 series, with n_{bb} labeled on graph. Master curves have been arbitrarily shifted for clarity.

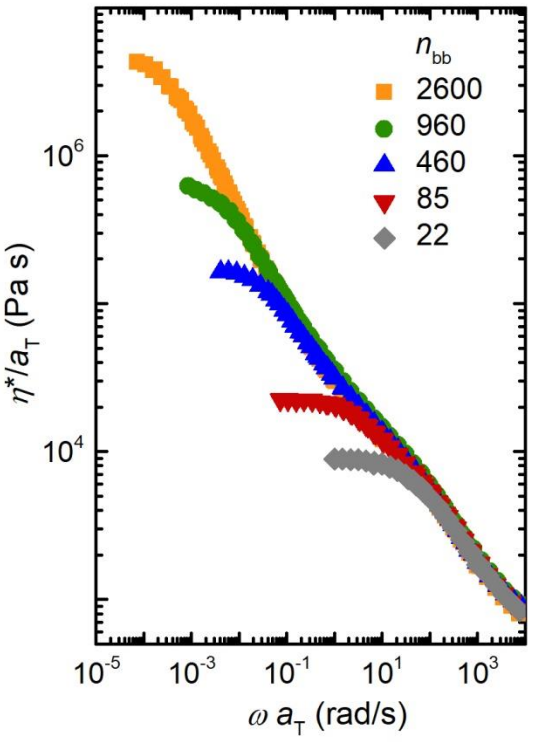

Figure S23. Reduced complex viscosity versus reduced frequency for z = 0.50series.

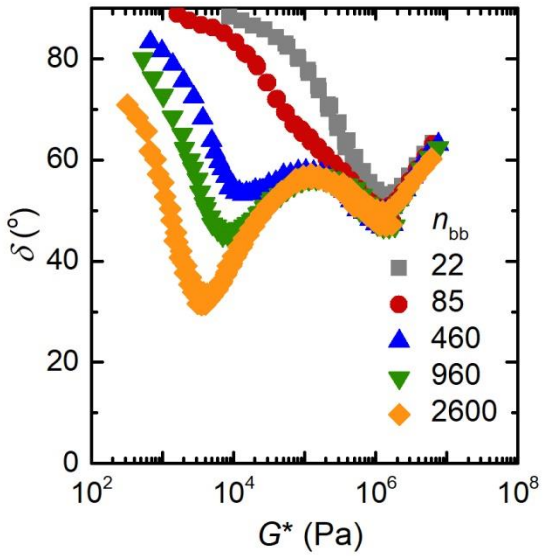

Figure S24. Van Gurp-Palmen plot for z = 0.50 series.

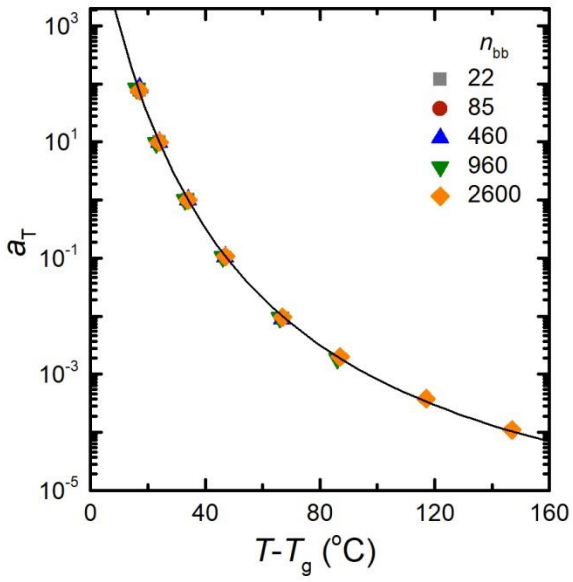

Figure S25. Shift factors for z = 0.50 polymers with WLF parameters C_1 = 6.7 and C_2 = 78 °C for $T_{ref} = T_g + 34$ °C.

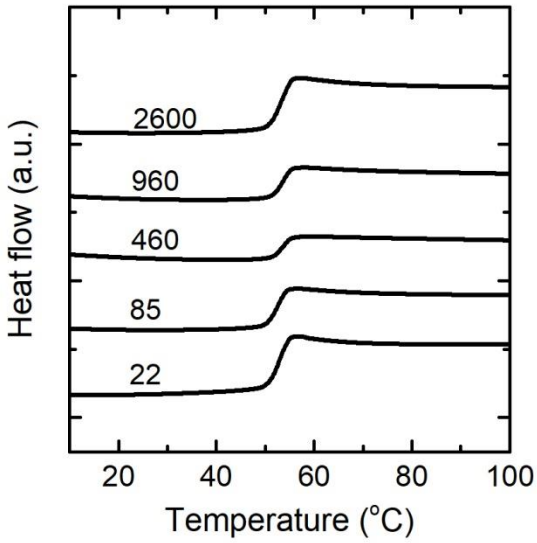

Figure S26. DSC traces for z = 0.50 series.

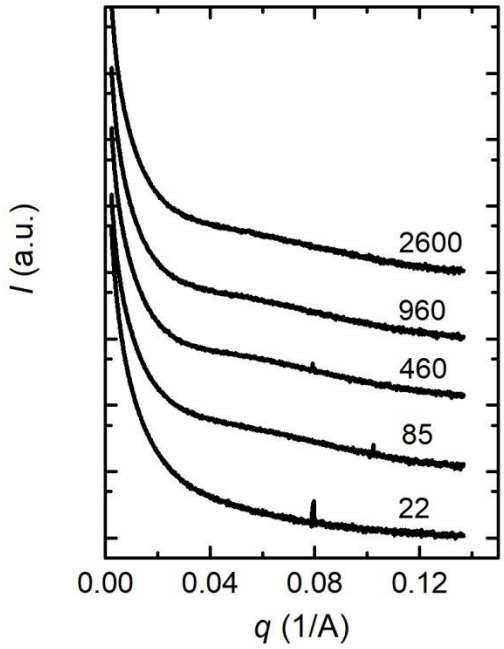

Figure S27. SAXS data for $z = 0.50$ series.

5.3 z = 0.40 data

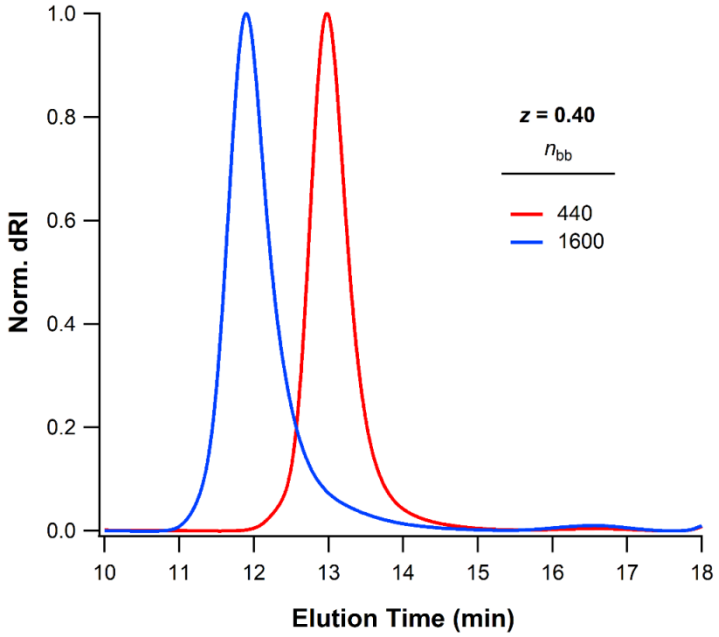

Figure S28. SEC data for all samples with z = 0.40.

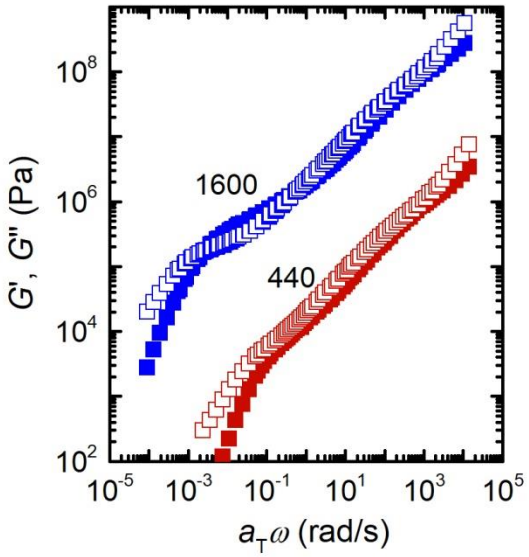

Figure S29. Master curves for z = 0.40 series, with n_{bb} labeled on graph. Master curves have been arbitrarily shifted for clarity.

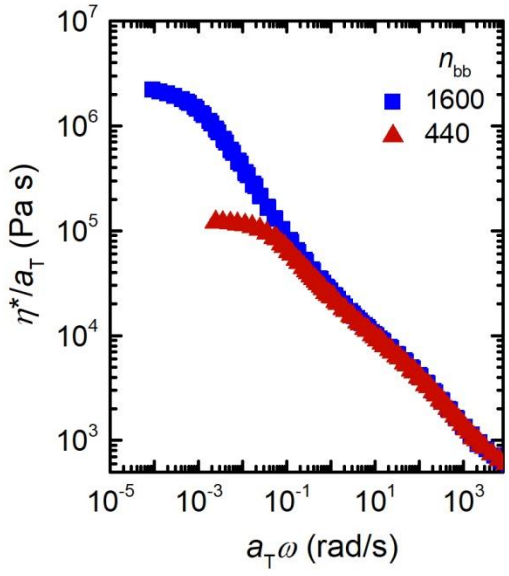

Figure S30. Reduced complex viscosity versus reduced frequency for z = 0.40 series.

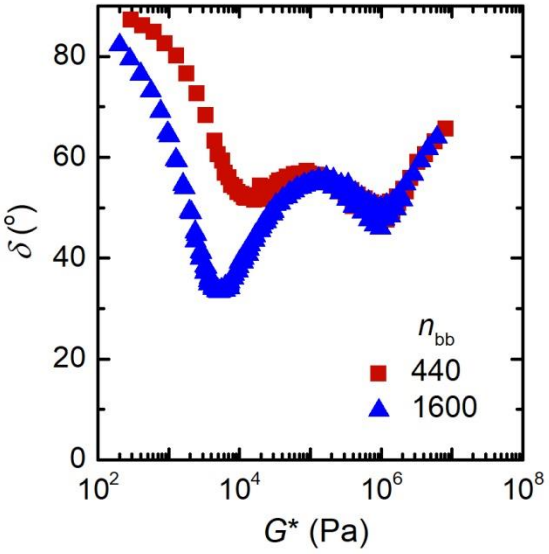

Figure S31. Van Gurp-Palmen plot for z = 0.40 series.

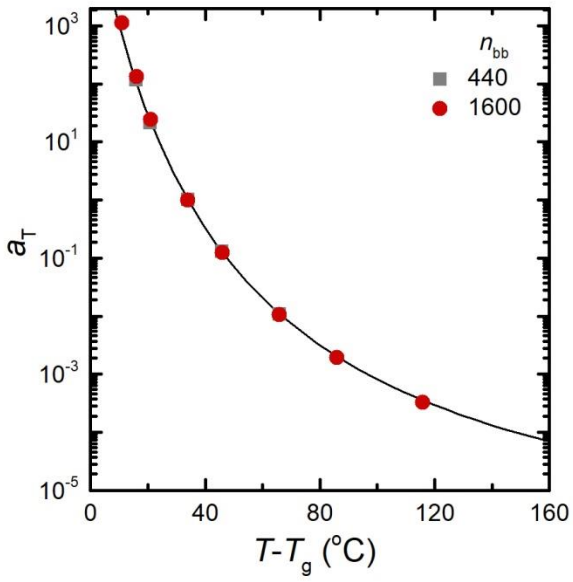

Figure S32. Shift factors for z = 0.40 polymers with WLF parameters C_1 = 6.7 and C_2 = 78 °C for T_{ref} = T_g + 34 °C.

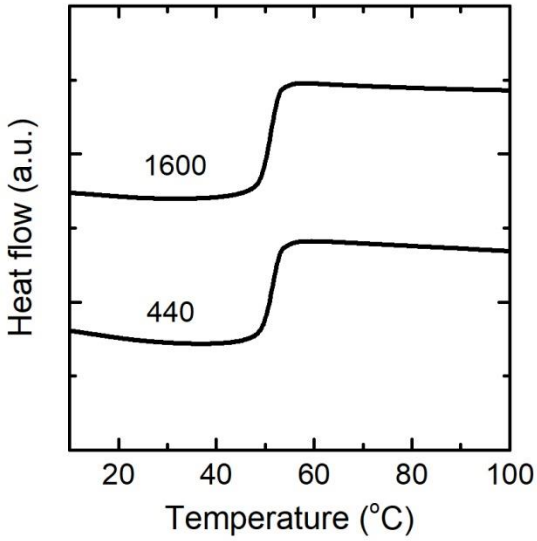

Figure S33. DSC traces for z = 0.40 series.

z = 0.40 samples were not included in SAXS experiments.

5.4 z = 0.25 data

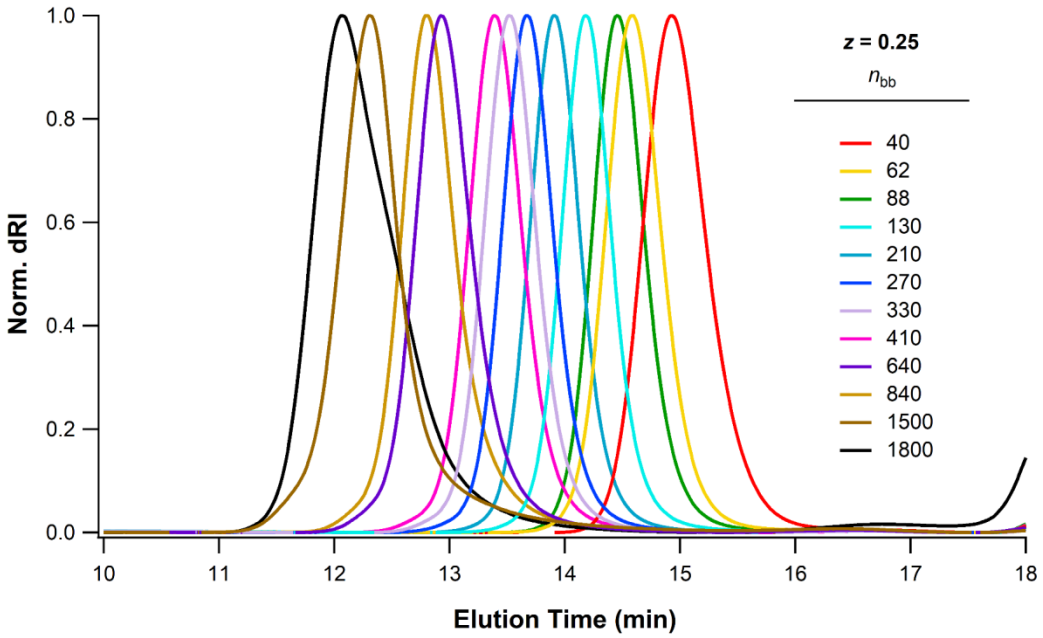

Figure S34. SEC data for all samples with z = 0.25.

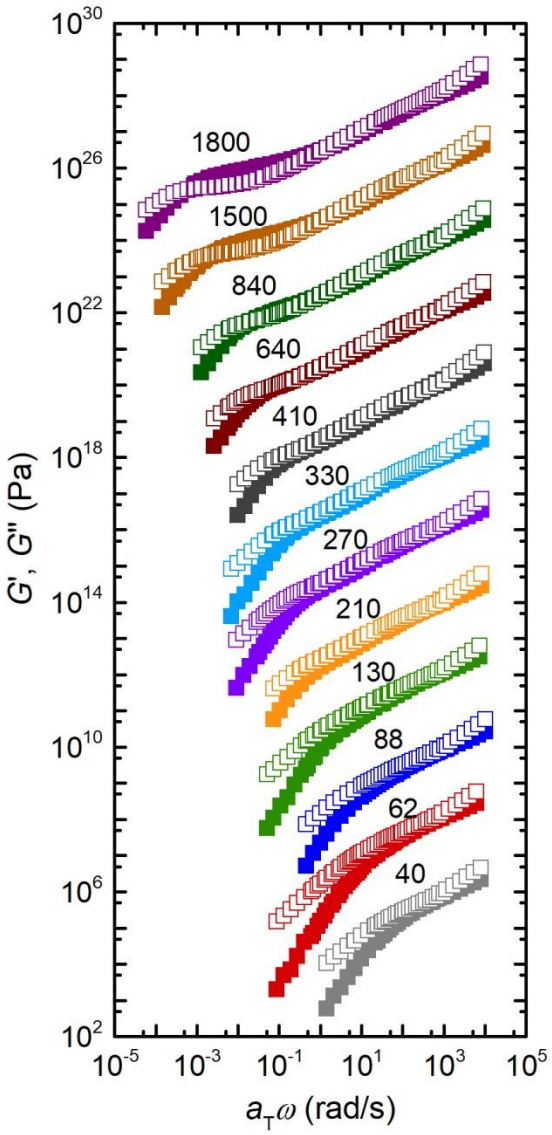

Figure S35. Master curve for z = 0.25 series, with n_{bb} labeled on graph. Master curves have been arbitrarily shifted for clarity.

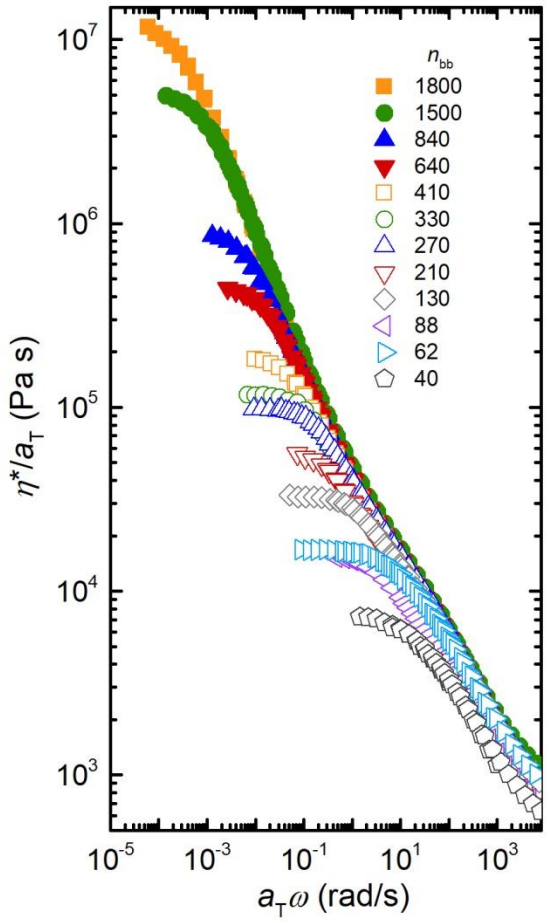

Figure S36. Reduced complex viscosity versus reduced frequency for z = 0.25series. Entangled samples are shown with closed symbols and unentangled samples are shown with open symbols.

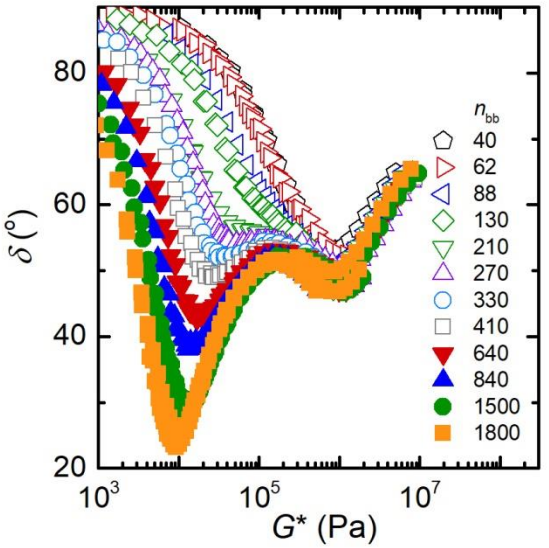

Figure S37. Van Gurp-Palmen plot for z = 0.25 series. Entangled samples are shown with closed symbols and unentangled samples are shown with open symbols.

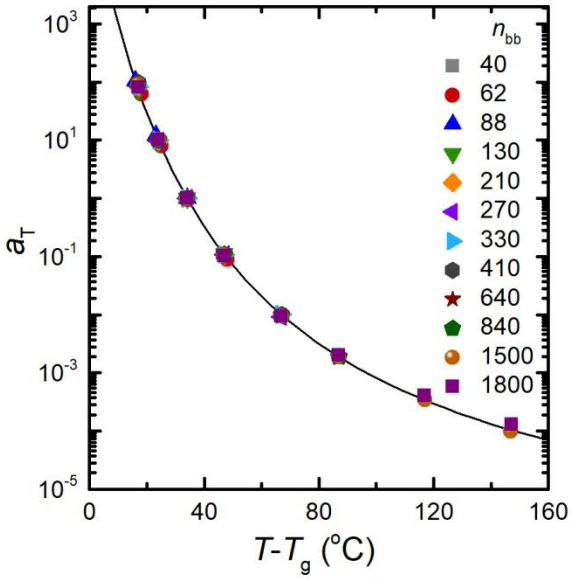

Figure S38. Shift factors for z = 0.25 polymers with WLF parameters C_1 = 6.7 and C_2 = 78 °C for $T_{ref} = T_g + 34$ °C.

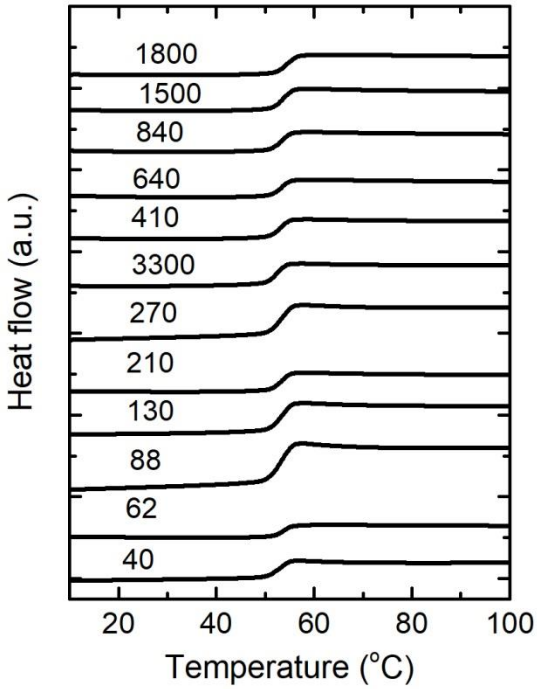

Figure S39. DSC traces for z = 0.25 series.

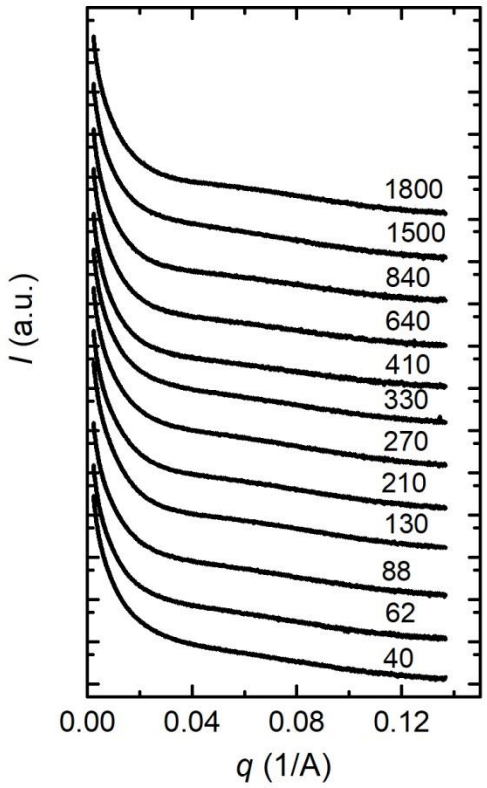

Figure S40. SAXS data for $z = 0.25$ series.

5.5 z = 0.20 data

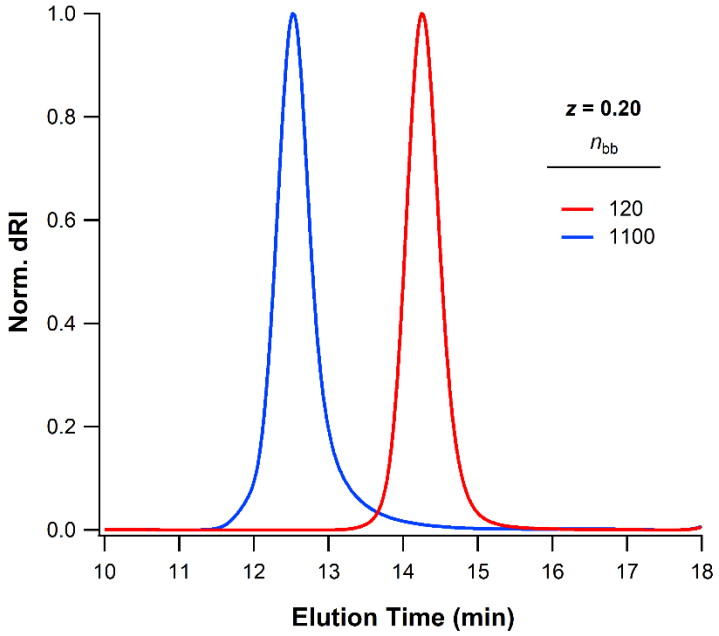

Figure S41. SEC data for all samples with z = 0.20.

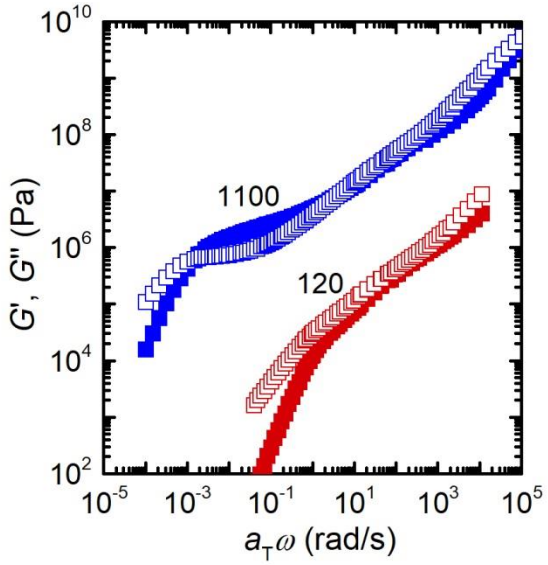

Figure S42. Master curve for z = 0.20 series, with n_{bb} labeled on graph. Master curves have been arbitrarily shifted for clarity.

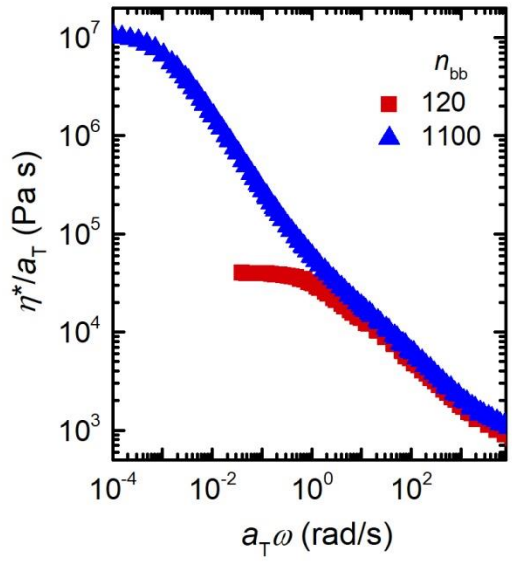

Figure S43. Reduced complex viscosity versus reduced frequency for z = 0.20 series.

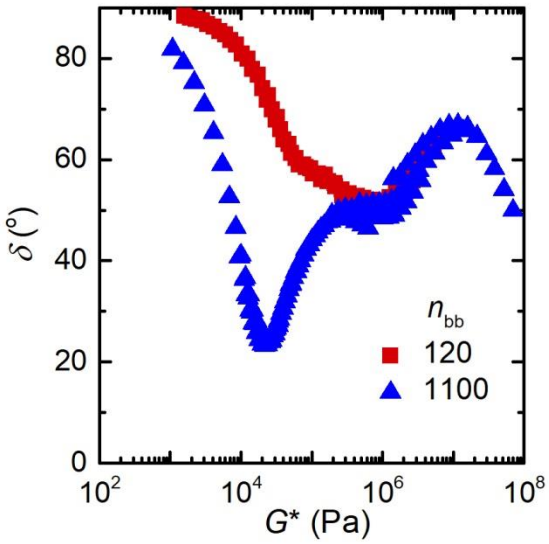

Figure S44. Van Gurp-Palmen plot for z = 0.20 series.

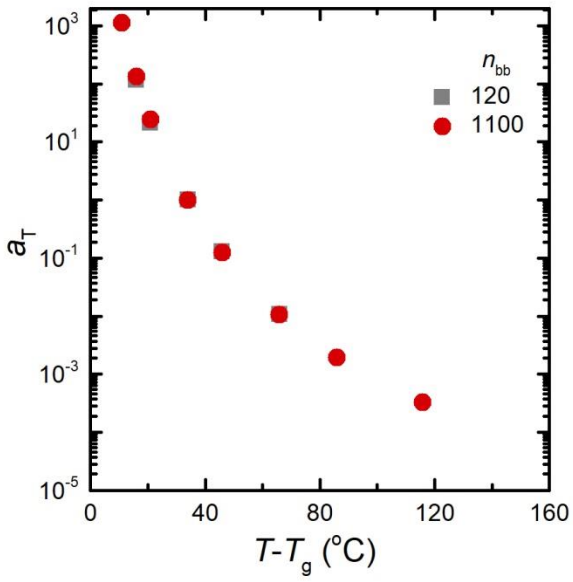

Figure S45. Shift factors for z = 0.20 polymers with WLF parameters C_1 = 6.7 and C_2 = 78 °C for T_{ref} = T_g + 34 °C.

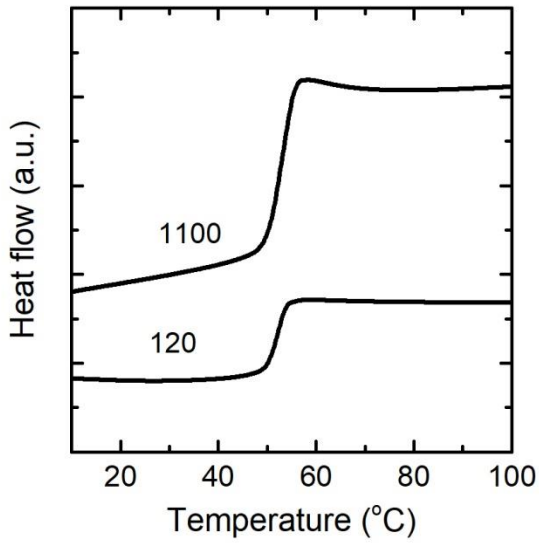

Figure S46. DSC traces for z = 0.20 series.

z = 0.20 samples were not included in SAXS experiments.

5.6 *z* = 0.15 data

The following data for the *z* = 0.15 series appears in Section 2: SEC (Figure S2), DSC (Figure S3), SAXS (Figure S4), van Gurp-Palmen plot (Figure S6), and reduced complex viscosity (Figure S8).

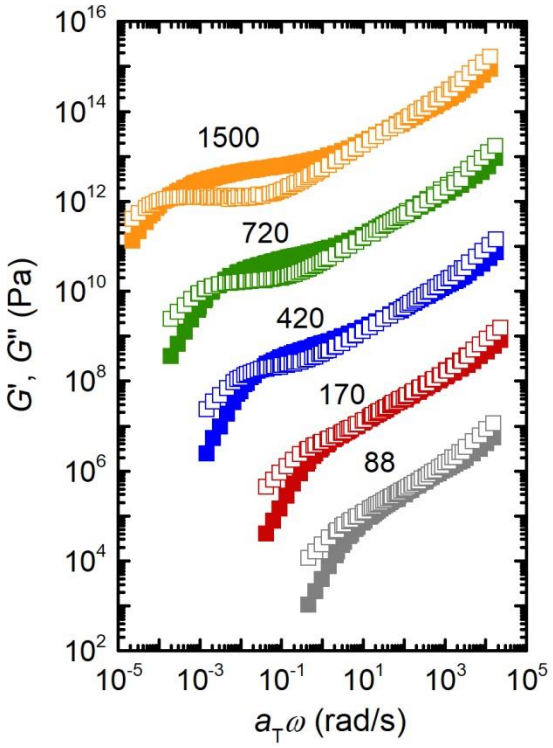

Figure S47. Master curve for *z* = 0.15 series, with n_{bb} labeled on graph. Master curves have been arbitrarily shifted for clarity.

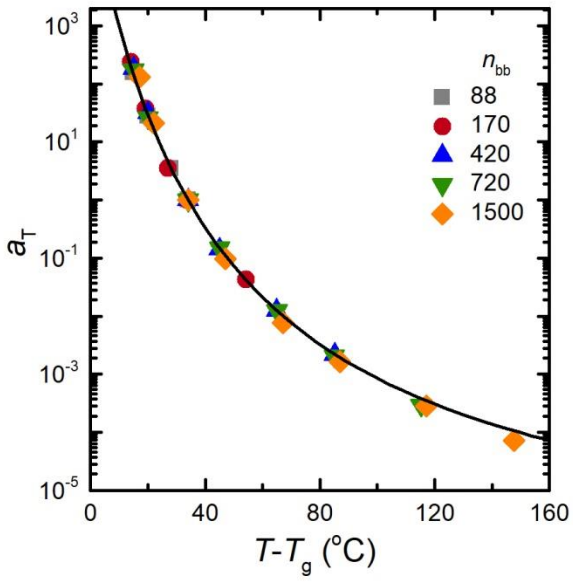

Figure S48. Shift factors for z = 0.15 polymers with WLF parameters C_1 = 6.7 and C_2 = 78 °C for $T_{ref} = T_g + 34$ °C.

5.7 *z* = 0.05data

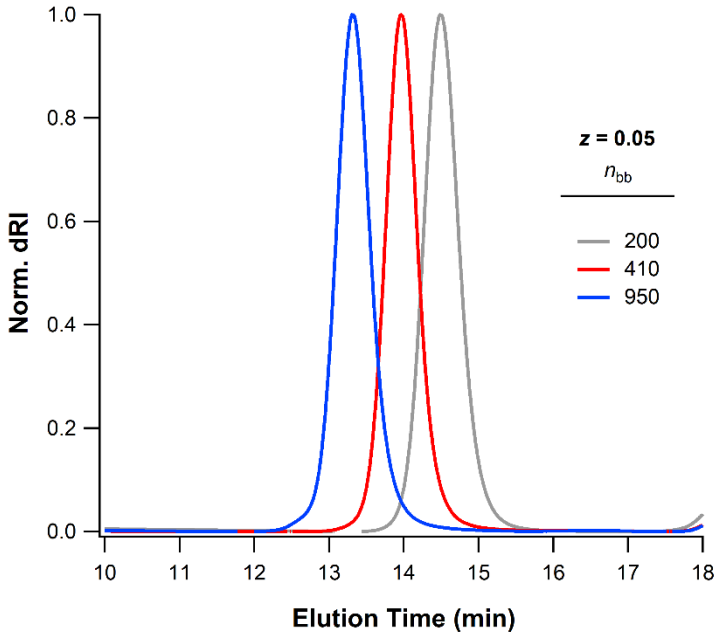

Figure S49. SEC data for all samples with *z* = 0.05.

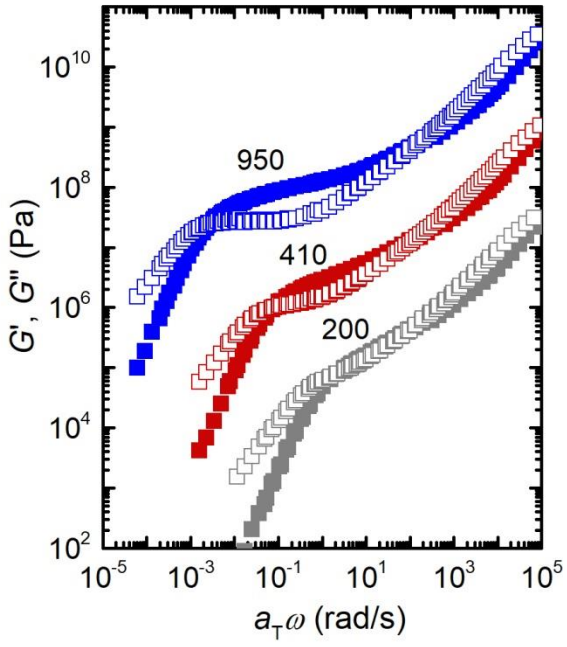

Figure S50. Master curves for *z* = 0.05 series, with n_{bb} labeled on graph. Master curves have been arbitrarily shifted for clarity.

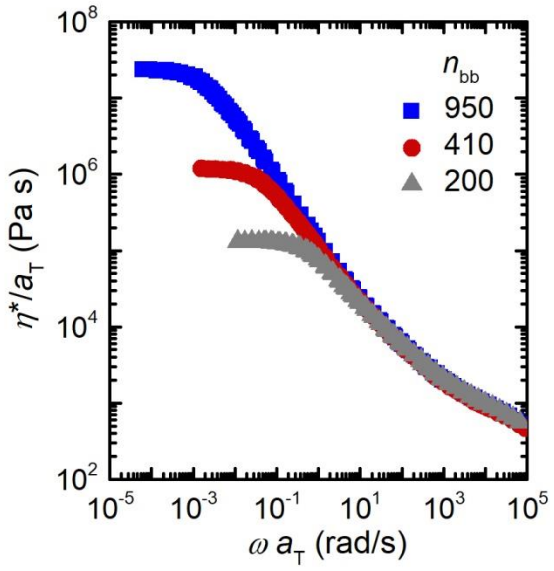

Figure S51. Reduced complex viscosity versus reduced frequency for z = 0.05 series.

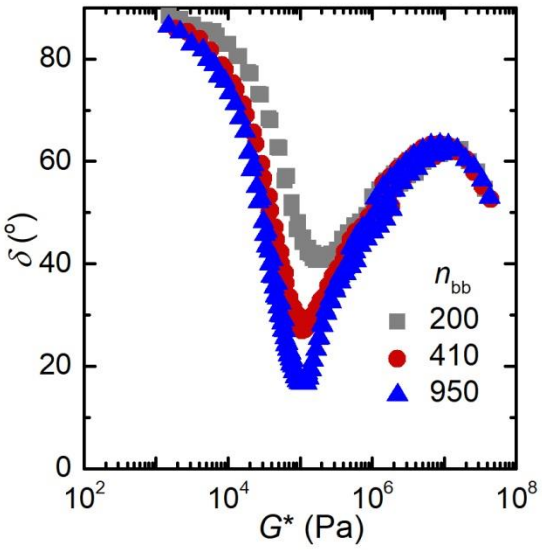

Figure S52. Van Gurp-Palmen plots for z = 0.05 series.

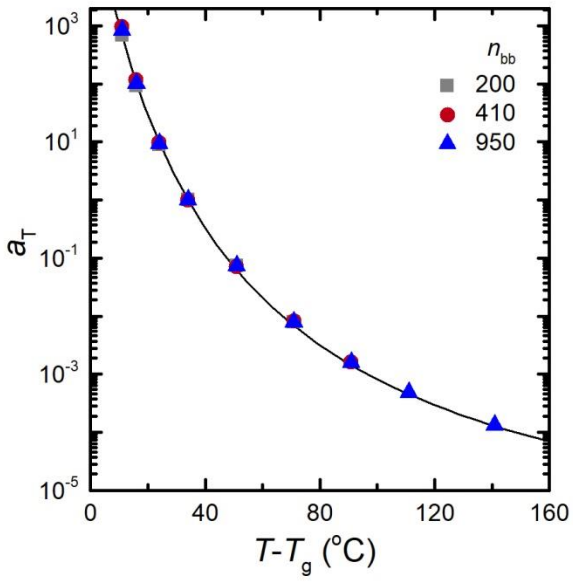

Figure S53. Shift factors for z = 0.05 polymers with WLF parameters C_1 = 6.7 and C_2 = 78 °C for $T_{ref} = T_g + 34$ °C.

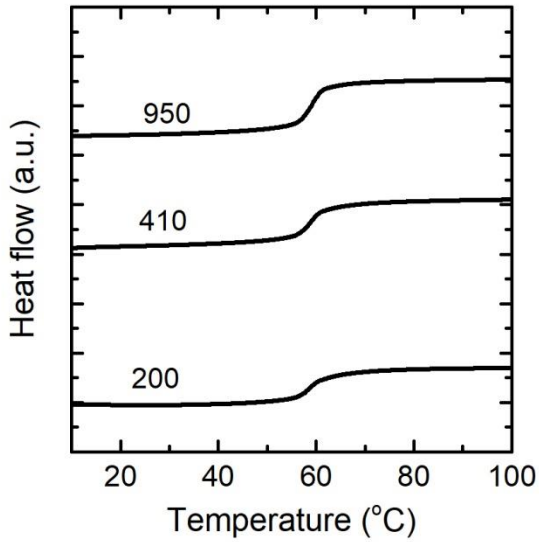

Figure S54. DSC traces for z = 0.05 series.

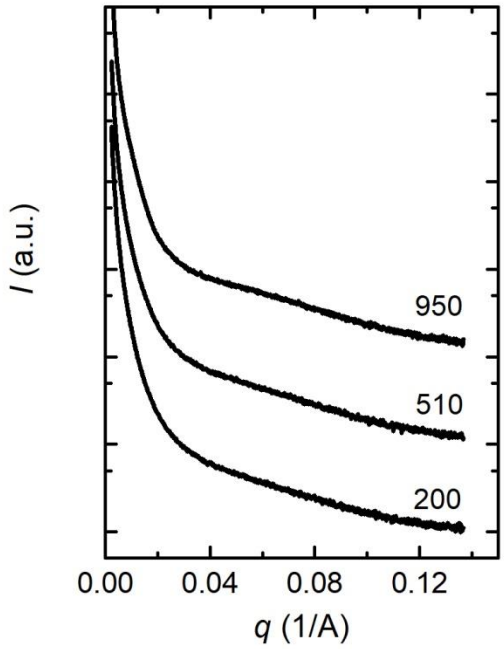

Figure S55. SAXS data for z = 0.05 series.

5.8 Linear DME (z = 0) data

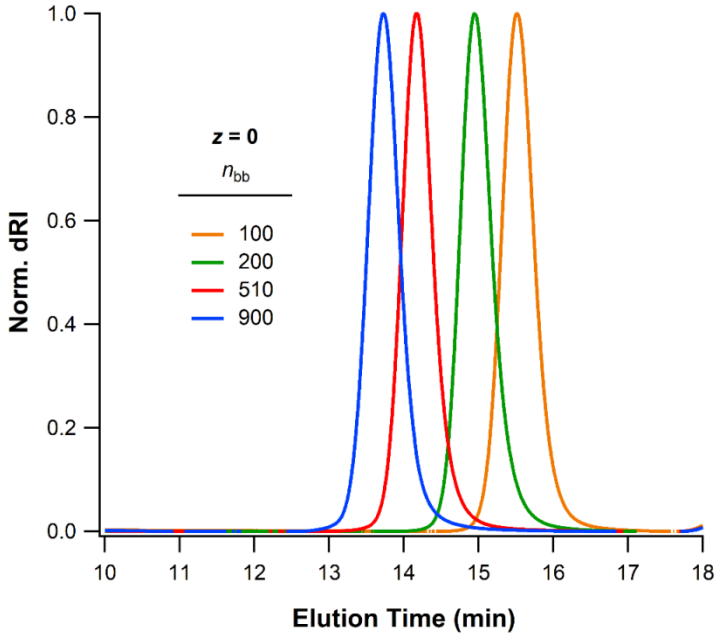

Figure S56. SEC data for all samples with z = 0.

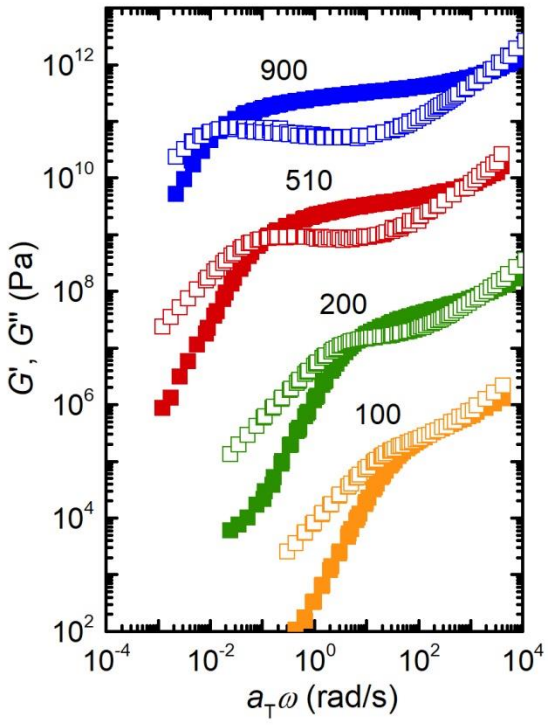

Figure S57. Master curves for linear DME series, with n_{bb} labeled on graph. Master curves have been arbitrarily shifted for clarity.

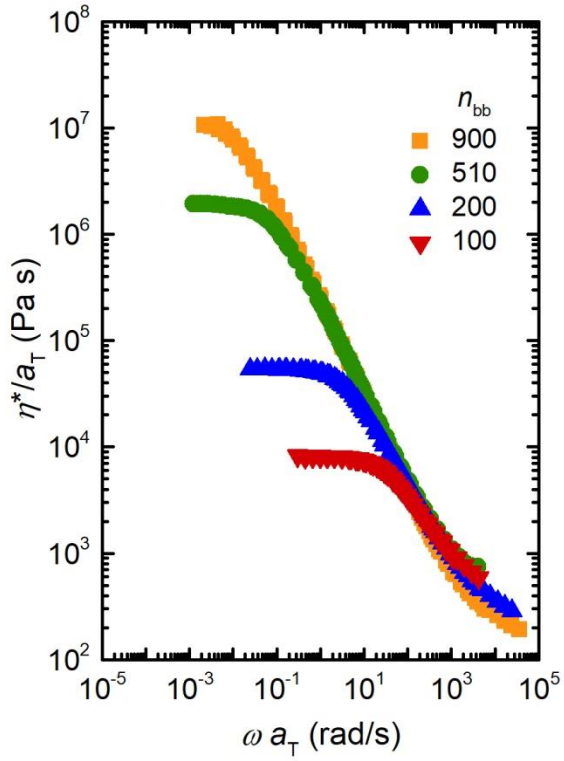

Figure S58. Reduced complex viscosity versus reduced frequency for linear DME series.

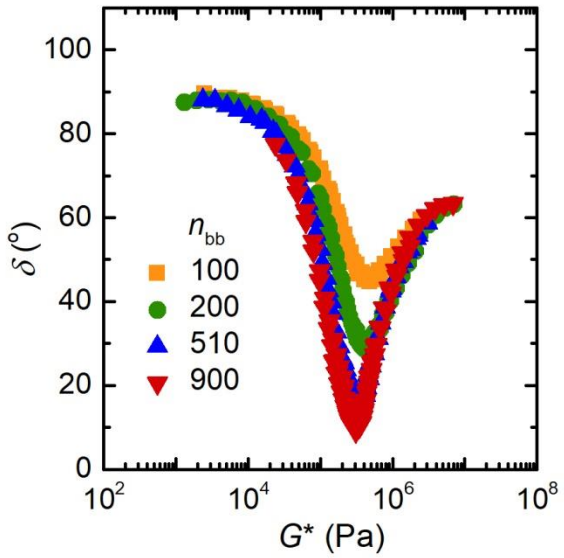

Figure S59. Van Gurp-Palmen plot for linear DME series.

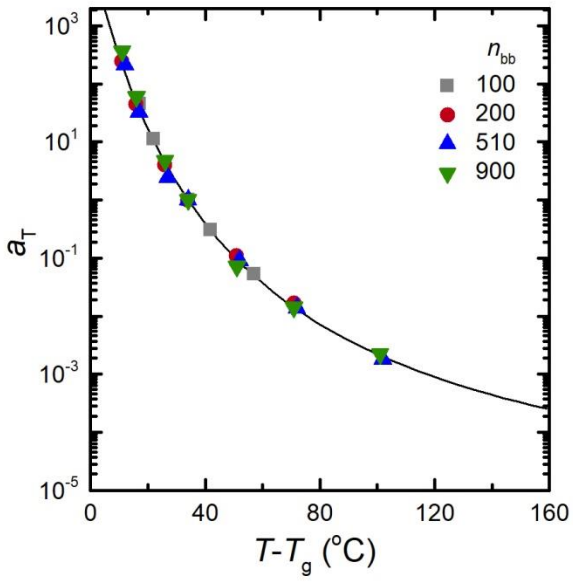

Figure S60. Shift factors for linear polymers with WLF parameters C_1 5.95 and C_2 = 82 °C for $T_{ref} = T_g + 34$ °C.

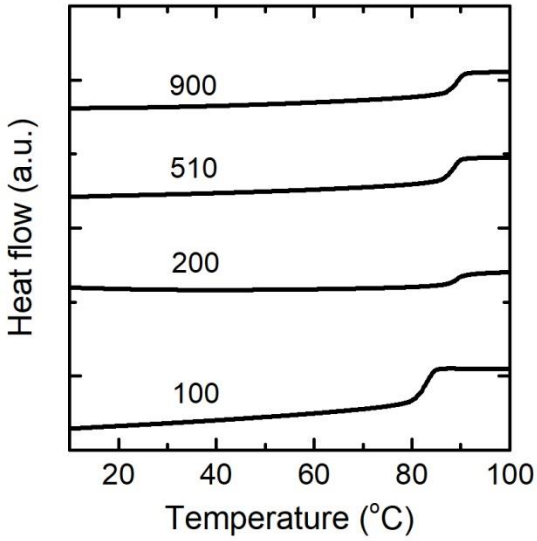

Figure S61. DSC traces for linear DME series.

Linear DME samples were not included in SAXS experiments.

6. References

(1) Love, J. A.; Morgan, J. P.; Trnka, T. M.; Grubbs, R. H. *Angew. Chem. Int. Ed.* **2002**, *41*, 4035–4037.

(2) Matson, J. B.; Grubbs, R. H. *J. Am. Chem. Soc.* **2008**, *130* (21), 6731–6733.

(3) Sveinbjornsson, B. R.; Weitekamp, R. A.; Miyake, G. M.; Xia, Y.; Atwater, H. A.; Grubbs, R. H. *Proc Natl Acad Sci USA* **2012**, *109*, 14332–14336.
(4) Lin, T.-P.; Chang, A. B.; Chen, H.-Y.; Liberman-Martin, A. L.; Bates, C. M.; Voegtle, M. J.; Bauer, C. A.; Grubbs, R. H. *J. Am. Chem. Soc.* **2017**, *139* (10), 3896–3903.
(5) Mezger, T. G. *The Rheology Handbook*, 4 ed.; Vincentz Network, 2014.
(6) Dalsin, S. J.; Hillmyer, M. A.; Bates, F. S. *Macromolecules* **2015**, *48* (13), 4680–4691.
(7) van Gurp, M.; Palmen, J. *Rheol. Bull.* **1998**, *67*, 5–8.
(8) Hu, M.; Xia, Y.; McKenna, G. B.; Kornfield, J. A.; Grubbs, R. H. *Macromolecules* **2011**, *44* (17), 6935–6943.
(9) Daniel, W. F. M.; Burdyńska, J.; Vatankhah-Varnoosfaderani, M.; Matyjaszewski, K.; Paturej, J.; Rubinstein, M.; Dobrynin, A. V.; Sheiko, S. S. *Nat Mater* **2016**, *15* (2), 183–189.
(10) Anderson, K. S.; Hillmyer, M. A. *Polymer* **2004**, *45* (26), 8809–8823.
(11) Dalsin, S. J.; Rions-Maehren, T. G.; Beam, M. D.; Bates, F. S.; Hillmyer, M. A.; Matsen, M. W. *ACS Nano* **2015**, *9* (12), 12233–12245.
(12) Fetters, L. J.; Lohse, D. J.; Richter, K.; Witten, T. A.; Zirkel, A. *Macromolecules* **1994**, *27*, 4639–4647.
(13) Lin, T.-P.; Chang, A. B.; Luo, S.-X.; Chen, H.-Y.; Lee, B.; Grubbs, R. H. *ACS Nano* **2017**, *11* (11), 11632–11641.